

SCATTERING OF SH-WAVES BY CIRCULAR AND ELLIPTICAL
CYLINDERS--A SOLUTION BY THE HILBERT-SCHMIDT METHOD

by

Hasan Tulgar

Submitted to the Faculty of Engineering
in Partial Fulfillment of
the Requirements for the Degree of
MASTER OF SCIENCE
in
MECHANICAL ENGINEERING

Bogazici University Library



39001100316507

14

BOĞAZIÇI UNIVERSITY

1981

47/05/

ABSTRACT

Near- and far-field solutions are presented for the scattering of SH-waves by a circular cavity and a rigid inclusion in infinite space while only far-field results are given for an elliptical geometry. Integral equations define the problem and these are solved in the spirit of Hilbert-Schmidt method. The results are given in graphical form and compared with the existing results.

Simple geometrical nature of the circle renders an exact solution whereas some approximations are needed to solve the scattering problem if the cross-section of the scatterer is in the shape of an ellipse. Here Bessel functions are used instead of Mathieu functions as is customary in literature concerning elliptical geometries. The results obtained are in fair agreement with the known exact solutions for up to $k \leq 1$ (k : wave number). If $k > 1$ only a good idea of the shape of the scattered wave could be obtained.

ÖZETCE

Skalar kayma dalgalarının (SH-dalgalarının) sonsuz ortamda dairesel bir boşluk ve rijit bir içcisimden saçılmasının yakın ve uzak bölge çözümleri verilmiştir. Eliptik geometri için ise sadece uzak bölge çözümleri elde edilmiştir. Problem entegral denklemlerle tanımlanmış ve çözümü için Hilbert-Schmidt metodu uygulanmıştır. Sonuçlar grafikler halinde sunulmuş olup, eldeki gerçek sonuçlarla kıyaslanmıştır.

Basit geometrisi dolayısı ile dairede kesin sonuç alınabilmesine karşın eliptik saçılma probleminin çözümü için bir takım yaklaşımlar kullanılmıştır. Literatürde bu tip problemlerin çözümünde genellikle "Mathieu" fonksiyonları kullanılmış olmasına rağmen bu çalışmada Bessel fonksiyonları tercih edilmiştir. Elde edilen sonuçlar $k \leq 1$ (k = dalga sayısı) için eldeki doğru çözümlere yakın olmakla beraber, $k > 1$ durumu için ancak saçılan dalganın şekli hakkında fikir edinilebilmiştir.

TABLE OF CONTENTS

I. Introduction	1
II. Equations of Elasticity and a method of analysis	
2.1 Dynamic Equations of Elasticity	4
2.2 Formulation of the Integral Equations	6
2.3 Method of Hilbert-Schmidt	21
III. Numerical Results	
3.1 Scattering by Circular Cylindrical Objects	
3.1.1 Scattering by a cavity	23
3.1.2 Scattering by a rigid inclusion	28
3.2 Scattering by an Elliptical Cylindrical Objects	
3.2.1 Scattering by a Cavity	31
3.2.2 Scattering by a rigid inclusion	39
IV. Discussion and Conclusion	44
Results	46
Appendix	81
Acknowledgements	85
References	86

CHAPTER I

INTRODUCTION

When a disturbance propagating in a medium encounters an object or any material discontinuity, it undergoes reflection and refraction thus producing new waves propagating inside and/or outside the object. This phenomenon is known as diffraction (scattering) of waves. Considerable work has been done over the past several years to obtain a thorough theoretical and experimental understanding of the scattering of elastic waves from defects of different geometries and material properties. The main goal is that once a complete understanding is obtained of the elastic waves scattered by known defects subsequent solution of the inverse problem, that is the identification of unknown defects in structural materials, will be possible. This is also known as non-destructive evaluation of materials.

The treatment of diffraction problems requires the solution to the linearized equations of elastodynamics subject to the boundary conditions on the surface of the scatterer. For a rigid body these conditions consist of the total displacement field on the surface of the body while for a cavity the vanishing of the surface tractions are required.

The literature concerning the diffraction of elastic waves is much less abundant for elliptic cylinders than for circular cylinders or spheres. The first paper we can trace is by Sezawa [1], in which the solution for the

scattering of a P-wave was given in terms of Mathieu functions. Later, Harumi [2] discussed the scattering of both P- and S-waves, and calculated the energy distribution of the wave scattered by a rigid ribbon, which is treated as the limiting case (infinite eccentricity) of a general ellipse.

The diffraction of acoustic or electromagnetic waves by an elliptical obstacle has been treated extensively. The formal solution in terms of Mathieu functions can be found in books by Mc Lachlan [3], and by Morse and Feshbach [4]. For the same geometric boundary, the analogous problem of the scattering of electric waves was investigated in 1897 by Rayleigh, [5], and in 1908 by Sieger, [6], who also contributed a great deal to the elliptic wave functions. The problem of sound waves was dealt with in 1938 by Morse and Rubenstein, [7], who first presented detailed numerical results for diffraction by a slit (degenerate ellipse). Subsequent publications were reviewed by Bouwkamp [8], and Jones [9]. Scattered wave-energy densities at low and medium frequency ranges were reported recently by Barakat [10].

An integral formulation for the problem of scattering of SH-waves will be presented in this work. As an alternate to the numerical methods, Hilbert-Schmidt theory will be used to solve these integral equations. In this method the field variables on the boundary of the scatterer are expressed in terms of infinite series with unknown coefficients which are determined using the boundary conditions.

The method will be applied to the scattering of SH-waves by circular and elliptical cylinders. Basically, the diffraction of waves by an elliptic cylinder is not much

different from that of a circular cylinder, especially when the eccentricity of the elliptical cross-section is small.

The Hilbert-Schmidt method is applicable only when the kernel of the integral equation can be represented by a series of orthogonal functions suitable for the geometry of the scatterer. In the case of an elliptic cylinder, these are Mathieu functions, which are difficult to evaluate numerically. Due to this difficulty, the basis functions of the circular case, namely Bessel functions, will be used instead of the Mathieu functions. Since the Bessel functions are easier to handle and more suitable to numerical computation, this choice aside from the elliptical case, allows one to deal with other shapes much more efficiently.

However, the numerical approximation of the integrals coupled with the truncation of the infinite series naturally introduces errors. Numerical results presented here agree well with the exact solutions for $k \leq 1$, whereas for $k > 1$ the solutions roughly resemble those of the exact solution.

In the following chapter, dynamic equations of elasticity and Hilbert-Schmidt method, for solving the scattering problem, are discussed. Formulation corresponding to circular and elliptical cavity and rigid inclusion are presented in Chapter III. Next the obtained results are discussed and finally they are shown in graphical form.

CHAPTER II

EQUATIONS OF ELASTICITY AND A METHOD OF ANALYSIS

2.1 Dynamic Equations of Elasticity

In a homogeneous, isotropic elastic medium, the displacement equations of motion is governed by the celebrated Navier's equation, i.e. [17]

$$(\lambda + \mu) \nabla (\nabla \cdot \underline{u}) + \mu \nabla^2 \underline{u} = \rho \frac{\partial^2 \underline{u}}{\partial t^2}$$

where λ and μ are the Lamé's constants with ρ being the mass density of the medium.

The scattering theory is based on the solution of the above equation subject to the appropriate boundary conditions prescribed over a discontinuity surface.

An anti-plane shear deformation is described by the displacement distribution [17]

$$u_x(x, y, t) = u_y(x, y, t) = 0 \quad \text{and} \quad u_z = u(x, y, t)$$

Only the z-component of the displacement vector survives and hence becomes a scalar quantity denoted by u . In this case the equations of motion reduce to a wave equation

$$\nabla^2 u(x, y, t) = \frac{1}{c^2} \frac{\partial^2 u(x, y, t)}{\partial t^2}$$

where $c = \sqrt{\mu/\rho}$ is the velocity of propagation of the

wave.

Considering only harmonic waves with a circular frequency w , we write

$$u(x,y,t) = U(x,y,w) e^{-iwt}$$

Substituting the above equation into the Navier's equation we get

$$\nabla^2 U + k^2 U = 0$$

where $k = w/c$ is the wave number. This equation is known as the Helmholtz equation.

Under the assumption of anti-plane strain, the dilatation $\nabla \cdot \underline{U}$ is zero, and the waves are rotational (S-waves). Because the displacement vector of the wave is always parallel to the z-axis, which for convenience can be taken as lying on a horizontal plane, waves of anti-plane strain are called SH-waves. Strictly speaking, the name manifests itself only when there is a direction which can be clearly labelled as horizontal.

2.2 Formulation of the integral equations

In this section a method for solving the wave diffraction problem is discussed namely the method of integral equation.

Consider two special functions $U(\underline{r}_0)$ and $G(\underline{r}, \underline{r}_0)$ which satisfy the following Helmholtz equations respectively.

$$(\nabla_0^2 + k^2) U(\underline{r}_0) = 0 \quad (2.1)$$

$$(\nabla_0^2 + k^2) G(\underline{r}, \underline{r}_0) = -\delta(\underline{r} - \underline{r}_0) \quad (2.2)$$

where $\underline{r}(x, y, z)$ and $\underline{r}_0(x_0, y_0, z_0)$ are the position vectors of the "observation points" and "source points" respectively. ∇^2 is the Laplacian operator in the "observing coordinates" x, y, z and ∇_0^2 the operator in "source coordinates" x_0, y_0, z_0 .

Multiplying equation (2.1) by $G(\underline{r}, \underline{r}_0)$, and equation (2.2) by $U(\underline{r}_0)$, and then subtracting the first from the second yields

$$U(\underline{r}_0) \nabla_0^2 G(\underline{r}, \underline{r}_0) - G(\underline{r}, \underline{r}_0) \nabla_0^2 U(\underline{r}_0) = -U(\underline{r}_0) \delta(\underline{r} - \underline{r}_0) \quad (2.3)$$

Integrating equation (2.3) over the volume with respect to source coordinates, see Fig.(2.1), we get

$$\iiint_V (U \nabla_0^2 G - G \nabla_0^2 U) dV_0 = - \iiint_V U \delta(\underline{r} - \underline{r}_0) dV_0 \quad (2.4)$$

Using the following relation:

$$\nabla_0 \cdot [n(\nabla_0 g)] = n(\nabla_0^2 g) + (\nabla_0 n) \cdot (\nabla_0 g) \quad (2.5)$$

the left hand side of the equation (2.4) can be written as

$$\iiint_V (U \nabla_0^2 G - G \nabla_0^2 U) dV_0 = \iiint_V \left\{ \nabla_0 \cdot ([U(\nabla_0 G)] - [G(\nabla_0 U)]) \right\} dV_0 \quad (2.6)$$

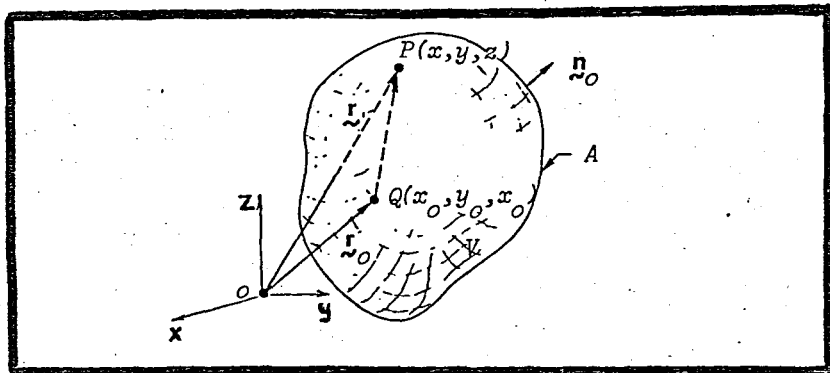


Fig. 2.1 Geometry of Observation Points $P(\underline{r})$ and Source Points $Q(\underline{r}_0)$ for the Interior Problem.

The right hand side of the equality given in equation (2.6) is in a form where we can use the Gauss's theorem [4]

$$\iiint_V \nabla_0 \cdot \underline{w} dV_0 = \iint_A \underline{w} \cdot \underline{n}_0 dA_0$$

where \underline{n}_0 is the unit outward normal to the surface A. Hence

(2.6) reduces to

$$\iiint_V (U \nabla_0^2 G - G \nabla_0^2 U) dV_0 = \iint_A \left(U \frac{\partial G}{\partial \bar{n}_0} - G \frac{\partial U}{\partial \bar{n}_0} \right) dA_0$$

where $(\partial/\partial n_0) = (\underline{n}_0 \cdot \nabla)$.

Substituting these results into equation (2.4) and employing the integral property of the delta function $\delta(\underline{r}-\underline{r}_0)$,

$$\iiint_V F(\underline{r}_0) \delta(\underline{r}-\underline{r}_0) dV_0 = \begin{cases} 0 & \underline{r} \text{ outside } V, \\ F(\underline{r}) & \underline{r} \text{ inside } V. \end{cases}$$

we get

$$\iint_A \left[G(\underline{r}, \underline{r}_0) \frac{\partial U(\underline{r}_0)}{\partial n_0} - U(\underline{r}_0) \frac{\partial G(\underline{r}, \underline{r}_0)}{\partial n_0} \right] dA_0 = \quad (2.7)$$

$$\begin{cases} U(\underline{r}) & \underline{r} \text{ inside } A, \\ 0 & \underline{r} \text{ outside } A. \end{cases}$$

The above equation is also known as the Helmholtz first (interior) formula.

Helmholtz's first formula is applicable in the case when all the singularities of the function $U(\underline{r})$ lie outside the surface A , shown in Fig. 2.1. (By a singularity of U , we mean a point at which U or one of its first and second partial derivative is discontinuous). If on the other hand, all the singularities of $U(\underline{r})$ lie within a closed surface A , we can apply Green's identity to the

region V bounded internally by A and externally by another closed surface B , a sphere with the center at the origin and a large radius R . (Fig. 2.2). The surface is now decomposed of A and B . Since $U(\underline{r})$ is assumed continuous outside A , application of Green's identity leads, as in equation (2.7), to

$$\iint_{A+B} \left[G(\underline{r}, \underline{r}_0) \frac{\partial U(\underline{r}_0)}{\partial n_0} - U(\underline{r}_0) \frac{\partial G(\underline{r}, \underline{r}_0)}{\partial n_0} \right] dA_0 = \quad (2.7a)$$

$$\begin{cases} U(\underline{r}) & \underline{r} \text{ inside } V, \\ 0 & \underline{r} \text{ outside } V. \end{cases}$$

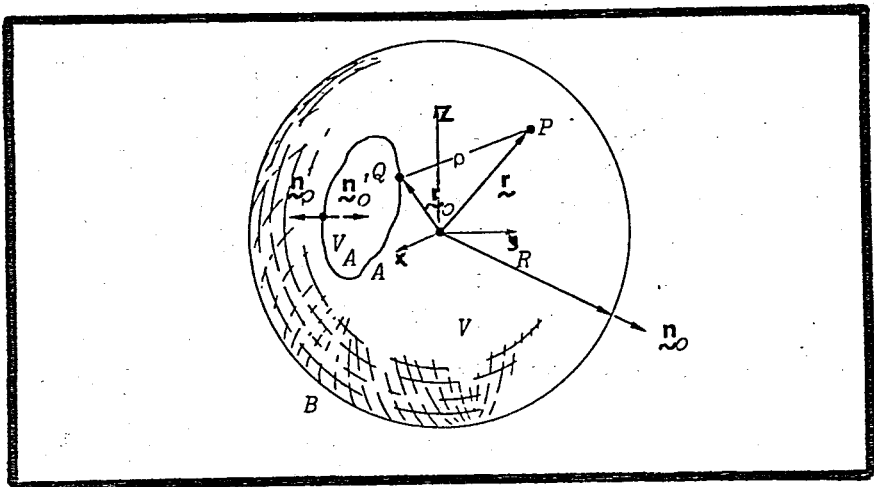


Fig. 2.2 Geometry for the Observation Point $P(\underline{r})$ and Source Point $Q(\underline{r}_0)$ for the Exterior Problem.

On the large surface B , we have $\underline{r}_0 = \underline{r}$, $\partial/\partial n_0 = \partial/\partial R$, and $dA = R^2 \sin\theta \, d\theta \, d\phi$. Noting that the Green's function in three dimensional problems is of the form [4]

$$G = \frac{e^{ik|R|}}{4\pi R} \quad (2.7b)$$

In the limit as $R \rightarrow \infty$, the integral over the surface B in equation (2.7a) using equation (2.7b) becomes

$$\lim_{R \rightarrow \infty} \iint_B \left(G \frac{\partial U}{\partial R} - U \frac{\partial G}{\partial R} \right) dA_0 =$$

$$\lim_{R \rightarrow \infty} \frac{1}{4\pi} \int_0^{2\pi} \int_0^\pi e^{ikR} \left[r_0 \left(\frac{\partial U}{\partial r_0} - ikU \right) + U \right]_{r_0=R} \sin\theta \, d\theta \, d\phi$$

The integral vanishes if, for any finite value M, the following relation hold,

$$|r_0 U| < M \quad , \quad \text{as } r_0 \rightarrow \infty$$

$$r_0 \left(\frac{\partial U}{\partial r_0} - ikU \right) \rightarrow 0 \quad , \quad \text{as } r_0 \rightarrow \infty \quad (2.8)$$

for all values of angular coordinates θ and ϕ . Equations (2.8) are known as the Sommerfeld radiation conditions.

Thus for a function $U(\underline{r})$ being regular in V, and satisfying Sommerfeld radiation conditions, its value at an observing point $P(\underline{r})$ is given by the surface integral over the source point $Q(\underline{r}_0)$ as

$$\iint_A \left[G(\underline{r}, \underline{r}_0) \frac{\partial U(\underline{r}_0)}{\partial n'_0} - U(\underline{r}_0) \frac{\partial G(\underline{r}, \underline{r}_0)}{\partial n'_0} \right] dA_0 =$$

$$\begin{cases} U(\underline{r}) & \underline{r} \text{ inside } V, \\ 0 & \underline{r} \text{ outside } V. \end{cases}$$

As shown in Fig. (2.2), the unit normal \underline{n}'_0 is away from the region V , and is an inward normal to the closed surface A . If an outer normal \underline{n}_0 to A is used, we have

$$\iint_A \left[U(\underline{r}_0) \frac{\partial G(\underline{r}, \underline{r}_0)}{\partial n_0} - G(\underline{r}, \underline{r}_0) \frac{\partial U(\underline{r}_0)}{\partial n_0} \right] dA_0 \quad (2.9)$$

$$\begin{cases} U(\underline{r}) & \underline{r} \text{ outside } A, \\ 0 & \underline{r} \text{ inside } A. \end{cases}$$

This is known as the Helmholtz second (exterior) formula.

The total wave $U^{(t)}$ in a medium is composed of two parts; the incident wave $U^{(i)}$ and scattered wave $U^{(s)}$, i.e.,

$$U^{(t)} = U^{(i)} + U^{(s)} \quad (2.10)$$

Each wave function satisfies the Helmholtz formula, (2.7) or (2.8). Let A be the surface of the scatterer with volume V_A (Fig. 2.3). We seek the solution for the total wave $U^{(t)}$ in the region V outside the surface A . The scattered wave function $U^{(s)}$, which represents physically

the waves radiated by secondary sources on or inside the surface A, usually is singular inside V_A . Thus Helmholtz's second formula is applicable with

$$\iint_A \left[U^{(s)}(\underline{r}_0) \frac{\partial G(\underline{r}, \underline{r}_0)}{\partial n_0} - G(\underline{r}, \underline{r}_0) \frac{\partial U^{(s)}(\underline{r}_0)}{\partial n_0} \right] dA_0 = \quad (2.11)$$

$$U^{(s)}(\underline{r}), \quad \underline{r} \text{ in } V$$

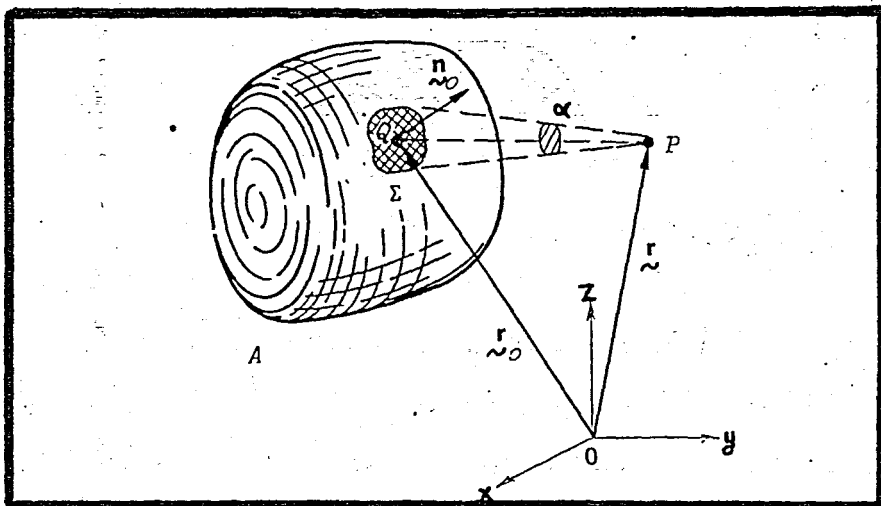


Fig. 2.3 Approach of the Observation Point $P(\underline{r})$ to the Source Point $Q(\underline{r}_0)$ on the Surface of a Scatterer with volume V_A and Bounding Surface A.

The derivative of $U^{(s)}(\underline{r})$ in V is obtained simply by differentiating the above equation:

$$\frac{\partial}{\partial n} \iint_A \left[U^{(s)}(\underline{r}_0) \frac{\partial G(\underline{r}, \underline{r}_0)}{\partial n_0} - G(\underline{r}, \underline{r}_0) \frac{\partial U^{(s)}(\underline{r}_0)}{\partial n_0} \right] dA_0 = \quad (2.12)$$

$$\frac{\partial}{\partial n} U^{(s)}(\underline{r}), \quad \underline{r} \text{ in } V$$

However, $U^{(s)}(\underline{r}_0)$ and $\partial U^{(s)}(\underline{r}_0)/\partial n_0$ are usually unknown for a given problem.

To find $U^{(s)}$ and its normal derivative on the surface A , we let the observation point $P(\underline{r})$ approach the source point $Q(\underline{r}_0)$ on the surface. With $\underline{r} \rightarrow \underline{r}_0$, equation (2.11) reduces to an integral equation for $U^{(s)}(\underline{r}_0)$ or $\partial U^{(s)}(\underline{r}_0)/\partial n_0$. However, because $\partial G(\underline{r}, \underline{r}_0)/\partial n_0$ is discontinuous across the surface A , the limits must be carried out with care. A general theorem for the continuity of $U^{(s)}$ and $\partial U^{(s)}/\partial n$ along a line normal to A can be constructed in a manner analogous to the integral theorems of potential functions. The following is a formal evaluation of the limits.

Consider at first the limit of the leading term on the left hand side of equation (2.11)

$$\lim_{\substack{\underline{r} \rightarrow \underline{r}_0^+ \\ \underline{r}_0 \rightarrow \underline{r}_0^+}} \iint_A U(\underline{r}_0) \frac{\partial G(\underline{r}, \underline{r}_0)}{\partial n_0} dA_0$$

The suffix (s) is dropped for the moment, and \underline{r}_0^+ indicates that the limit is approached from the positive side of the normal \underline{n}_0 . Since $\partial G(\underline{r}, \underline{r}_0)/\partial n_0$ is singular at $\underline{r} = \underline{r}_0$, we exclude the source point from the surface.

integral by encircling it with a small area Σ . In the neighborhood of $Q(\underline{r}_0)$, the Green's function for the wave equation (Equation 2.7b), can be approximated by its static value

$$G(\underline{r}, \underline{r}_0) = \frac{1}{4\pi|\underline{r}-\underline{r}_0|}$$

Hence,

$$\begin{aligned} \lim_{r \rightarrow r_0^+} \iint_A U(\underline{r}_0) \frac{\partial G(\underline{r}, \underline{r}_0)}{\partial n_0} dA_0 &= \\ &= \frac{1}{4\pi} \lim_{\underline{r} \rightarrow \underline{r}_0^+} \iint_{\Sigma} U(\underline{r}_0) \frac{\partial}{\partial n_0} \frac{1}{|\underline{r}-\underline{r}_0|} dA_0 + \\ &+ \lim_{r \rightarrow r_0^+} \iint_{A-\Sigma} U(\underline{r}_0) \frac{\partial G(\underline{r}, \underline{r}_0)}{\partial n_0} dA_0 \end{aligned}$$

The limit of the second term on the right can be evaluated directly because $\partial G / \partial n_0$ is continuous at $A-\Sigma$. For the first term, one notes that

$$\frac{\partial}{\partial n_0} \frac{1}{|\underline{r}-\underline{r}_0|} dA_0 = \frac{\underline{n}_0 \cdot (\underline{r}-\underline{r}_0)}{|\underline{r}-\underline{r}_0|^3} dA_0 = d\alpha(\underline{r}, \underline{r}_0),$$

where $d\alpha$ is the solid angle subtended by the surface dA_0 . With a smooth surface at \underline{r}_0 , one then obtains

$$\lim_{\underline{r} \rightarrow \underline{r}_0^+} \iint_{\Sigma} U(\underline{r}_0) \frac{\partial}{\partial n_0} \frac{1}{|\underline{r} - \underline{r}_0|} dA_0 = U(\underline{r}_0) \lim_{\underline{r} \rightarrow \underline{r}_0^+} \iint_{\Sigma} d\alpha = 2\pi U(\underline{r}_0)$$

The final answer is then

$$\lim_{\underline{r} \rightarrow \underline{r}_0^+} \iint_A U(\underline{r}_0) \frac{\partial G(\underline{r}, \underline{r}_0)}{\partial n_0} dA_0 = \frac{1}{2} U(\underline{r}_0) +$$

$$\text{P.V.} \iint_A U(\underline{r}_0) \frac{\partial G(\underline{r}, \underline{r}_0)}{\partial n_0} dA_0, \quad \underline{r} = \underline{r}_0 \quad (2.13)$$

where P.V. designates the principal value of the integral as defined by

$$\text{P.V.} \iint_A F(x, y) dx dy = \lim_{\Sigma \rightarrow 0} \iint_{A-\Sigma} F(x, y) dx dy \quad (2.14)$$

The limit of the second integral in (2.11) as $\underline{r} \rightarrow \underline{r}_0^+$ can be evaluated directly if the unknown function $\partial U^{(s)}(\underline{r}_0) / \partial n_0$ satisfies the Hölder condition⁽¹⁾.

(1) A function $f(\underline{r})$ is said to satisfy the Hölder condition at \underline{r}_0 if there are three positive constants a, b and c such that

$$|f(\underline{r}) - f(\underline{r}_0)| \leq a |\underline{r} - \underline{r}_0|^c$$

for all points \underline{r} for which $|\underline{r} - \underline{r}_0| < b$. When $0 \leq c \leq 1$, this is known as the Lipschitz condition.

Thus as $\underline{r} \rightarrow \underline{r}_0^+$, equation (2.11) reduces to

$$\frac{1}{2} U^{(s)}(\underline{r}) = \iint_A \left[U^{(s)}(\underline{r}_0) \frac{\partial G(\underline{r}, \underline{r}_0)}{\partial n_0} - G(\underline{r}, \underline{r}_0) \frac{\partial U^{(s)}(\underline{r}_0)}{\partial n_0} \right] dA_0, \quad \underline{r} \text{ on } A \quad (2.15)$$

The statement " \underline{r} on A " means that \underline{r} is set equal to \underline{r}_0 after integration, where \underline{r}_0 are the coordinates of the surface points, and the principal value of the integral is to be taken whenever it becomes necessary. Applying the same limiting process to equation (2.12) we get

$$\frac{1}{2} \frac{\partial U^{(s)}(\underline{r})}{\partial n} = \frac{\partial}{\partial n} \iint_A \left[U^{(s)}(\underline{r}_0) \frac{\partial G(\underline{r}, \underline{r}_0)}{\partial n_0} - G(\underline{r}, \underline{r}_0) \frac{\partial U^{(s)}(\underline{r}_0)}{\partial n_0} \right] dA_0, \quad \underline{r} \text{ on } A \quad (2.16)$$

Equation (2.15) and (2.16) show that the wave function $U^{(s)}(\underline{r}_0)$ and its normal derivative $\partial U^{(s)}(\underline{r}_0)/\partial n_0$ are not independent of each other on the surface. If

$\partial U^{(s)}(\underline{r}_0)/\partial n_0$ is known at A , $U^{(s)}(\underline{r}_0)$ must satisfy the integral equation (2.15) which is of the second kind of Fredholm-type integral equation (2.16). On the other hand, if the $U^{(s)}$ is prescribed at the surface A , $\partial U^{(s)}(\underline{r}_0)/\partial n_0$ is then determined by equation (2.15), which becomes a Fredholm integral equation of the first

kind.

In many problems, the boundary values are prescribed in terms of the total wave function $U^{(t)}$ or $\partial U^{(t)} / \partial n$. It is then more convenient to derive a set of integral equations for the total wave. This can be done easily by noting that the incident wave $U^{(i)}$, which has no singularity inside the boundary A , hence satisfies the Helmholtz first formula

$$\iint_A \left[G(\underline{r}, \underline{r}_0) \frac{\partial U^{(i)}(\underline{r}_0)}{\partial n_0} - U^{(i)}(\underline{r}_0) \frac{\partial G(\underline{r}, \underline{r}_0)}{\partial n_0} \right] dA_0 = 0$$

\underline{r} in V .

Adding the above equality to equation (2.11) and using (2.10), one finds

$$U^{(i)}(\underline{r}) + \iint_A \left[U^{(t)}(\underline{r}_0) \frac{\partial G(\underline{r}, \underline{r}_0)}{\partial n_0} - G(\underline{r}, \underline{r}_0) \frac{\partial U^{(t)}(\underline{r}_0)}{\partial n_0} \right] dA_0 = U^{(t)}(\underline{r}), \quad \underline{r} \text{ in } V \quad (2.17)$$

By letting \underline{r} approach to \underline{r}_0 as in equation (2.15), or by differentiating it and then taking the limit as in equation (2.16), it is easy to obtain

$$U^{(i)}(\underline{r}) + \iint_A \left[U^{(t)}(\underline{r}_o) \frac{\partial G(\underline{r}, \underline{r}_o)}{\partial n_o} - G(\underline{r}, \underline{r}_o) \frac{\partial U^{(t)}(\underline{r}_o)}{\partial n_o} \right] dA_o = \frac{1}{2} U^{(t)}(\underline{r}), \quad \underline{r} \text{ on } A \quad (2.18)$$

$$\frac{\partial U^{(i)}(\underline{r})}{\partial n} + \frac{\partial}{\partial n} \iint_A \left[U^{(t)}(\underline{r}_o) \frac{\partial G(\underline{r}, \underline{r}_o)}{\partial n_o} - G(\underline{r}, \underline{r}_o) \frac{\partial U^{(t)}(\underline{r}_o)}{\partial n_o} \right] dA_o = \frac{1}{2} \frac{\partial U^{(t)}(\underline{r})}{\partial n}, \quad \underline{r} \text{ on } A \quad (2.19)$$

Again the integrals are evaluated in the sense of principal values. Solutions of equations (2.15), (2.16), (2.18), or (2.19) yield the values of $U^{(s)}$ or $U^{(t)}$, or their normal derivatives, at the boundary A , from which the values of the corresponding quantities in the region V outside A can be obtained using the equations (2.11) or (2.17).

Two special boundary conditions are to be noted. One is that the total field $U^{(t)}$ vanishes on the surface A , that is $U^{(s)} = -U^{(i)}$. This is usually referred to as Dirichlet's condition.

The second special boundary condition is that the normal derivative of $U^{(t)}$ vanishes on the surface A , or

equivalently, $\frac{\partial U^{(s)}}{\partial n} = - \frac{\partial U^{(i)}}{\partial n}$. This is known as Neumann's condition.

For either of these two types of boundary conditions, the integral equations are greatly simplified and are listed below.

(1) Dirichlet Condition $U^{(t)} = 0$, $(U^{(s)} = -U^{(i)})$ on A. Equation (2.18) reduces to

$$U^{(i)}(\underline{r}) = \iint_A G(\underline{r}, \underline{r}_o) \frac{\partial U^{(t)}(\underline{r}_o)}{\partial n_o} dA_o, \quad \underline{r} \text{ on A} \quad (2.20)$$

Similarly equation (2.19) becomes

$$\frac{\partial U^{(i)}(\underline{r})}{\partial n} = \frac{1}{2} \frac{\partial U^{(t)}(\underline{r})}{\partial n} + \iint_A \frac{\partial G(\underline{r}, \underline{r}_o)}{\partial n} \frac{\partial U^{(t)}(\underline{r}_o)}{\partial n_o} dA_o, \quad \underline{r} \text{ on A} \quad (2.21)$$

(2) Neumann Condition $\partial U^{(t)} / \partial n = 0$ on A. Equation (2.19) and (2.18) becomes

$$- \frac{\partial U^{(i)}(\underline{r})}{\partial n} = \frac{\partial}{\partial n} \iint_A U^{(t)}(\underline{r}_o) \frac{\partial G(\underline{r}, \underline{r}_o)}{\partial n_o} dA_o, \quad \underline{r} \text{ on A} \quad (2.22)$$

$$U^{(i)}(\underline{r}) = \frac{1}{2} U^{(t)}(\underline{r}) - \iint_A U^{(t)}(\underline{r}_o) \frac{\partial G(\underline{r}, \underline{r}_o)}{\partial n_o} dA_o, \quad ,$$

\underline{r} on A

(2.23)

respectively.

2.3 Method of Hilbert-Schmidt

The Fredholm integral equation of the first kind for $T(\underline{r})$

$$f(\underline{r}) = \iint_A G(\underline{r}, \underline{r}_0) T(\underline{r}_0) dA_0, \quad \underline{r} \text{ on } A \quad (2.24)$$

can be solved if the kernel $G(\underline{r}, \underline{r}_0)$ can be expanded into a series of orthogonal functions suitable for the surface A . Let $S_n(\underline{r})$ ($n=1, 2, 3, \dots$) be the orthogonal functions which satisfies the wave equation and the orthogonality condition

$$\iint_A S_n(\underline{r}) S_m(\underline{r}) w(\underline{r}) dA = \begin{cases} 1 & (m=n) \\ 0 & (m \neq n) \end{cases}, \quad (2.25)$$

where $w(\underline{r})$ is a weighting function. Suppose $G(\underline{r}, \underline{r}_0)$ also admits the following series expansion

$$G(\underline{r}, \underline{r}_0) = \sum_{n=1}^{\infty} b_n S_n(\underline{r}) S_n(\underline{r}_0)$$

We then expand the given function $f(\underline{r})$ and the unknown function $T(\underline{r}_0)$ into two series of the form

$$f(\underline{r}) = \sum_n a_n S_n(\underline{r})$$

$$T(\underline{r}_0) = \left[\sum_m c_m S_m(\underline{r}_0) \right] w(\underline{r}_0)$$

By substituting the three series in the integral equation,

One obtains

$$\sum_n a_n S_n(\vec{r}) = \sum_n \sum_m \left[c_m b_n S_n(\vec{r}) \iint_A w(\vec{r}_0) S_n(\vec{r}_0) S_m(\vec{r}_0) \right] dA_0$$

\vec{r} on A

which, in view of the orthogonality condition, fixes the unknown coefficient c_n as

$$c_n = a_n / b_n, \quad n=1,2,\dots$$

This, in essence, is the Hilbert-Schmidt's method, and its applications to particular problems will be given in the following sections.

CHAPTER III

NUMERICAL RESULTS

3.1 Scattering by Circular Cylindrical Objects

3.1.1 Scattering by a Cavity

Consider a circular cylindrical cavity in an infinitely extended solid as shown in Fig.(3.1). The cylinder has a radius of a . Let a SH-wave propagating in the positive x -direction be incident on it. The wave will be scattered by the cylinder, and the question is to find the scattered wave form, both on the boundary of the cavity and outside, i.e., $r \geq a$.

Equation (2.22) in two-dimensional case becomes

$$-\frac{\partial U^{(i)}(\underline{r})}{\partial n} = \frac{\partial}{\partial n} \int_{\Gamma} U^{(t)}(\underline{r}_0) \frac{\partial G(\underline{r}, \underline{r}_0)}{\partial n_0} dS_0 \quad (2.22')$$

where in the two dimensional case the Green's function is [4]

$$G(\underline{r}, \underline{r}_0) = (i/4) H_0^{(1)}(k|\underline{r} - \underline{r}_0|).$$

In the cylindrical coordinates (r, θ) , one can write [4]

$$G(\underline{r}, \underline{r}_0) = (i/4) \sum_{m=0}^{\infty} \cos m(\theta - \theta_0) \begin{cases} J_m(kr_0) H_m^{(1)}(kr) & , r > r_0 \\ J_m(kr) H_m^{(1)}(kr_0) & , r < r_0 \end{cases} \quad (3.1)$$

where $J_m(z)$ and $H_m^{(1)}(z)$ are the m -th order Bessel function and Hankel function of the first kind respectively.

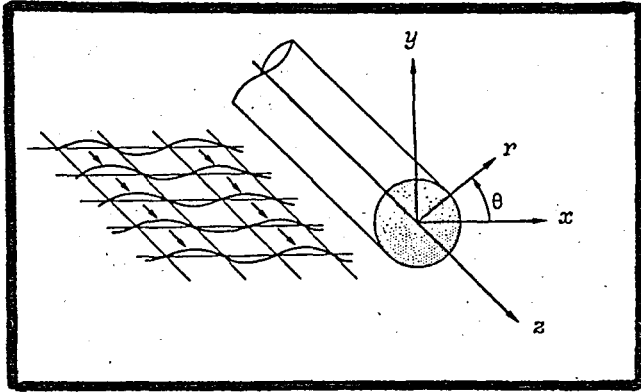


Fig. 3.1 Circular Cylindrical Cavity
and Incident Simple Harmonic
SH-waves

The incident SH-wave along the x -axis is represented by [14]

$$U^{(i)}(\underline{r}) = U_0 \sum_{m=0}^{\infty} \epsilon_m i^m J_m(kr) \cos m\theta \quad (3.2)$$

where U_0 is the amplitude of the wave and $\epsilon_0 = 1$ and $\epsilon_m = 2$ for $m=1, 2, 3, \dots$

Assuming that $U^{(t)}$ on the surface of the scatterer can be written in the form

$$U^{(t)}(\underline{r}_0) = \sum_{n=0}^{\infty} B_n \cos n \theta_0 \quad (3.3)$$

equation (2.22') takes the form

$$-\frac{\partial U^{(i)}(\underline{r})}{\partial n} = (i/4) \frac{\partial}{\partial n} \int_0^{2\pi} \left(\sum_{n=0}^{\infty} B_n \cos n \theta_0 \right) \left[\sum_{m=0}^{\infty} J'_m(ka) H_m^{(1)}(kr) \cos m(\theta - \theta_0) \right] a d\theta_0 \quad (3.4)$$

where prime indicates differentiation with respect to r_0 . Note that

$$\int_0^{2\pi} \cos m(\theta - \theta_0) \cos n\theta_0 d\theta_0 = \begin{cases} 0 & , m \neq n \\ \pi \cos n\theta & , m = n \end{cases} \quad (3.5)$$

Equation (3.4) together with (3.2) becomes

$$-U_0 \sum_{m=0}^{\infty} \epsilon_m i^m J'_m(ka) \cos m\theta_0 = (i\pi a/4) \sum_{n=0}^{\infty} B_n J'_n(ka) H_n^{(1)'}(ka) \cos n\theta_0$$

Using the orthogonality condition for the circular function, $\cos n\theta$, in the above equation, we get

$$B_n = \frac{-\epsilon_n i^n U_0}{(i\pi a/4) H_n^{(1)'}(ka)}$$

Once the value of $U^{(t)}$ over the surface A ($r=a$) is known, the scattered wave in the field $r > a$ can be calculated from (2.17) since $U^{(s)} = U^{(t)} - U^{(i)}$ where

$\partial U^{(t)}(\underline{r}_0)/\partial n = 0$ for a cavity.

$$\begin{aligned}
 U^{(s)}(\underline{r}) &= \int_0^{2\pi} U^{(t)}(\underline{r}_0) \frac{\partial G(\underline{r}, \underline{r}_0)}{\partial n_0} a \, d\theta_0 \\
 &= -\frac{U_0}{\pi} \int_0^{2\pi} \left\{ \left(\sum_{n=0}^{\infty} \frac{\epsilon_n i^n}{H_n^{(1)}(ka)} \cos n\theta_0 \right) \right. \\
 &\quad \left. \left[\sum_{m=0}^{\infty} J_m'(ka) H_m^{(1)}(kr) \cos m(\theta - \theta_0) \right] \right\} a \, d\theta_0
 \end{aligned}$$

Using equation (3.5) again, we get

$$U^{(s)}(\underline{r}) = -U_0 \sum_{n=0}^{\infty} \epsilon_n i^n \frac{J_n'(ka)}{H_n^{(1)'}(ka)} H_n^{(1)}(kr) \cos n\theta$$

Hence, in the case of a cavity, the total field outside the scatterers is

$$U^{(t)}(\underline{r}) = U^{(i)}(\underline{r}) + U^{(s)}(\underline{r})$$

$$= U_0 \sum_{n=0}^{\infty} \epsilon_n i^n \left[J_n(kr) - \frac{J_n'(ka)}{H_n^{(1)'}(ka)} H_n^{(1)}(kr) \right] \cos n\theta$$

Numerical results for the displacement and the tangential stress fields on the boundary of the scatterer, due to the scattered waves are presented in Figures 1 and 3 respectively for different values of ka . We also present

the distribution of the displacement at the far field
($r/a = 2000$) in Figures 2.

3.1.2 Scattering by a rigid inclusion

In the case of scattering by a rigid inclusion, the total wave field $U^{(t)}$ on the boundary Γ satisfies the integral equation

$$U^{(i)}(\underline{r}) = \int_{\Gamma} G(\underline{r}, \underline{r}_0) \frac{\partial U^{(t)}(\underline{r}_0)}{\partial n_0} dS_0, \quad \underline{r} \text{ on } \Gamma \quad (2.20')$$

If we assume the normal derivative of the total wave field at $\underline{r}_0 = a$ to be of the form

$$\frac{\partial U^{(t)}(\underline{r}_0)}{\partial n_0} = \sum_{n=0}^{\infty} B_n \cos n\theta_0 \quad (3.6)$$

equation (2.20') can be written as

$$\begin{aligned} U^{(i)}(\underline{r}) &= (i/4) \int_0^{2\pi} \left\{ \left(\sum_{n=0}^{\infty} B_n \cos n\theta_0 \right) \right. \\ &\quad \left. \left[\sum_{m=0}^{\infty} J_m(ka) H_m^{(1)}(kr) \cos m(\theta - \theta_0) \right] \right\} a d\theta_0 \\ &= (i\pi a/4) \sum_{n=0}^{\infty} B_n J_n(ka) H_n^{(1)}(kr) \cos n\theta, \quad \underline{r} \text{ on } \Gamma \end{aligned}$$

Similar to the cavity case, replacing $U^{(i)}(\underline{r}_0)$ by its series representation, the unknown coefficients B_n can be shown to be

$$B_n = \frac{-4 i^{n+1} \epsilon_n}{\pi a H_n^{(1)}(ka)} U_0 \quad (3.7)$$

Knowing the value for $\partial U^{(t)} / \partial n$ at the surface A, ($r=a$), the scattered waves in the region $r>a$ can be calculated from equation (2.17), i.e.,

$$U^{(i)}(\underline{r}) + \iint_A \left[U^{(t)}(\underline{r}_0) \frac{\partial G(\underline{r}, \underline{r}_0)}{\partial n_0} - G(\underline{r}, \underline{r}_0) \frac{\partial U^{(t)}(\underline{r}_0)}{\partial n_0} \right] dA_0 = U^{(t)}(\underline{r})$$

Using the boundary condition $U^{(t)}(\underline{r}_0) = 0$ and noting that $U^{(s)}(\underline{r}) = U^{(t)}(\underline{r}) - U^{(i)}(\underline{r})$, the above equation in two dimensions reduces to

$$U^{(s)}(\underline{r}) = - \int_{\Gamma} G(\underline{r}, \underline{r}_0) \frac{\partial U^{(t)}(\underline{r}_0)}{\partial n_0} dS_0, \quad \underline{r} \text{ in } \Gamma \quad (3.8)$$

Substituting equations (3.6), (3.7) and using the series representation for the Green's function in the above equation, and carrying out the integrals we get

$$\begin{aligned}
 U^{(s)}(\underline{r}) &= - (i\pi a/4) \sum_{n=0}^{\infty} B_n J_n(ka) H_n^{(1)}(kr) \cos n\theta \\
 &= - U_0 \sum_{n=0}^{\infty} \epsilon_n i^n \left[J_n(ka)/H_n^{(1)}(ka) \right] H_n^{(1)}(kr) \cos n\theta
 \end{aligned}
 \tag{3.9}$$

Numerical examples regarding the far field displacements and the normal stress distribution on the boundary of the scatterer due to the scattered waves are shown in Figures 4 and 5 respectively. For far field calculations r/a is taken to be 2000.

3.2 Scattering by an Elliptical Cylindrical Object

3.2.1 Scattering by a Cavity

From equation (2.22'), it is seen that, the total wave $U^{(t)}$ on the boundary Γ for the problem of scattering by a cavity satisfies the integral equation

$$-\frac{\partial U^{(i)}(\underline{r})}{\partial n} = \frac{\partial}{\partial n} \int_{\Gamma} U^{(t)}(\underline{r}_0) \frac{\partial G(\underline{r}, \underline{r}_0)}{\partial n_0} dS_0 \quad (2.22')$$

The normal derivative of the Green's function $G(\underline{r}, \underline{r}_0)$ in the above equation using chain rule, becomes

$$\frac{\partial G}{\partial n_0} = \frac{\partial G}{\partial r_0} \frac{\partial r_0}{\partial n_0} \quad (3.10)$$

where in cylindrical coordinates (r, θ) from equation (3.1)

$$\frac{\partial G(\underline{r}, \underline{r}_0)}{\partial r_0} = (i/4) \sum_{m=0}^{\infty} \cos m(\theta - \theta_0) \begin{cases} J'_m(kr_0) H_m^{(1)}(kr) & , r > r_0 \\ J_m(kr) H_m^{(1)'}(kr_0) & , r < r_0 \end{cases} \quad (3.11)$$

the primes indicating differentiation with respect to r_0 . The boundary of an elliptical scatterer, in polar coordinates is given by the relation

$$r_0 = \frac{ab}{\sqrt{a^2 \sin^2 \theta_0 + b^2 \cos^2 \theta_0}} \quad (3.12)$$

Hence, the derivative of r_0 with respect to the outward normal n_0 is

$$\frac{\partial r_0}{\partial n_0} = \frac{b^2 \cos^2 \theta_0 + a^2 \sin^2 \theta_0}{\sqrt{b^4 \cos^2 \theta_0 + a^4 \sin^2 \theta_0}} \quad (3.13)$$

where a and b are the major and minor axes of the ellipse. A detailed derivation of the above expressions (3.12) and (3.13) are given in Appendix.

The integral in equation (2.22') over the arc length can now be transformed into an integral over the angle θ_0 using the relation

$$dS_0 = ab \sqrt{\frac{a^4 \sin^2 \theta_0 + b^4 \cos^2 \theta_0}{(a^2 \sin^2 \theta_0 + b^2 \cos^2 \theta_0)^3}} d\theta_0 \quad (3.14)$$

see Appendix for the details. Hence, using equation (3.3) and the equations (3.10) thru (3.14) in equation (2.22'), we get

$$-\frac{\partial U^{(i)}(\underline{r})}{\partial n} = (i/4) \frac{\partial}{\partial n} \int_0^{2\pi} \left[\left(\sum_{n=0}^{\infty} B_n \cos n\theta_0 \right) \left[\sum_{m=0}^{\infty} J_m(kr) H_m^{(1)'}(kr_0) \cos m(\theta - \theta_0) \frac{ab}{\sqrt{a^2 \sin^2 \theta_0 + b^2 \cos^2 \theta_0}} \right] \right] d\theta_0 \quad (3.15)$$

Utilizing the trigonometric identity

$$\cos n\theta_0 \cos m(\theta - \theta_0) =$$

$$1/2 \cos m\theta \left[\cos (m+n) \theta_0 + \cos (m-n) \theta_0 \right] + \quad (3.16)$$

$$1/2 \sin m\theta \left[\sin (m+n) \theta_0 + \sin (m-n) \theta_0 \right]$$

equation (3.15) yield

$$\begin{aligned} -\frac{\partial U^{(i)}(r)}{\partial n} &= (i/8) \frac{\partial}{\partial n} \sum_{p=0}^{\infty} \sum_{m=0}^{\infty} B_p \cos m\theta J_m'(kr) \\ &\quad \int_0^{2\pi} [\cos(m+p)\theta_0 + \cos(m-p)\theta_0] \frac{H_m^{(1)'}(kr_0) ab d\theta_0}{\sqrt{a^2 \sin^2 \theta_0 + b^2 \cos^2 \theta_0}} \\ &+ (i/8) \frac{\partial}{\partial n} \sum_{p=0}^{\infty} \sum_{m=0}^{\infty} B_p \sin m\theta J_m'(kr) \\ &\quad \int_0^{2\pi} [\sin(m+p)\theta_0 + \sin(m-p)\theta_0] \frac{H_m^{(1)'}(kr_0) ab d\theta_0}{\sqrt{a^2 \sin^2 \theta_0 + b^2 \cos^2 \theta_0}} \end{aligned} \quad (3.17)$$

Defining

$$A_{pm} \equiv \int_0^{2\pi} [\cos(m+p)\theta_0 + \cos(m-p)\theta_0] \frac{H_m^{(1)'}(kr_0) ab d\theta_0}{\sqrt{a^2 \sin^2 \theta_0 + b^2 \cos^2 \theta_0}}$$

$$C_{pm} \equiv \int_0^{2\pi} [\sin(m+p)\theta_0 + \sin(m-p)\theta_0] \frac{H_m^{(1)'}(kr_0) ab d\theta_0}{\sqrt{a^2 \sin^2 \theta_0 + b^2 \cos^2 \theta_0}}$$

(3.18)

Equation (3.17) can be written as

$$-\frac{\partial U^{(i)}(\underline{r})}{\partial n} = (i/8) \frac{\partial r}{\partial n} \sum_{n=0}^{\infty} \sum_{m=0}^{\infty} B_{nm} J_m'(kr) [A_{pm} \cos m\theta + C_{pm} \sin m\theta] \quad (3.19)$$

where prime indicates differentiation with respect to r .

Recalling equation (3.2) the normal derivative of the incident field on the boundary can be written as

$$\frac{\partial U^{(i)}(\underline{r}_0)}{\partial n_0} = U_0 \frac{\partial r_0}{\partial n_0} \sum_{m=0}^{\infty} \epsilon_m i^m J_m'(kr_0) \cos m\theta_0.$$

Hence, equation (3.19) evaluated on the boundary becomes

$$-U_0 \sum_{m=0}^{\infty} \epsilon_m i^m J_m'(kr_0) \cos m\theta_0 = (i/8) \sum_{n=0}^{\infty} \sum_{m=0}^{\infty} B_{nm} J_m'(kr_0) (A_{nm} \cos m\theta_0 + C_{nm} \sin m\theta_0) \quad (3.20)$$

Note that θ_0 appears implicitly in the argument of the $J'_m(kr_0) - r_0$ is a function of θ_0 - the well known orthogonality condition for $\cos m\theta_0$ doesn't apply here to solve equation (3.20) for the unknown coefficients B_n . Since equation (3.20) is true for all θ_0 between 0° and 360° , one can take $\theta_0 = 0^\circ$. This choice simplifies equation (3.20) to

$$-U_0 \sum_{m=0}^{\infty} \epsilon_m i^m J'_m(kr_0) = (i/8) \sum_{n=0}^{\infty} \sum_{m=0}^{\infty} J'_m(kr_0) B_n A_{nm} \quad (3.21)$$

Substituting the relation [18]

$$J'_m(kr_0) = \frac{kr_0}{2} \left[J_{m-1}(kr_0) - J_{m+1}(kr_0) \right]$$

into equation (3.21), yields

$$\begin{aligned} -U_0 \sum_{m=0}^{\infty} \epsilon_m i^m \left[J_{m-1}(kr_0) - J_{m+1}(kr_0) \right] = \\ (i/8) \sum_{n=0}^{\infty} \sum_{m=0}^{\infty} B_n A_{nm} \left[J_{m-1}(kr_0) - J_{m+1}(kr_0) \right] \end{aligned} \quad (3.22)$$

Recall the orthogonality condition [19]

$$\int_0^{\infty} t^{-1} J_{v+2n+1}(t) J_{v+2m+1}(t) dt = \begin{cases} 0 & (m \neq n) \\ \frac{1}{2(2n+v+1)} & (m = n) \quad (v+n+m > -1) \end{cases} \quad (3.23)$$

Multiplying equation (3.22) by $J_s(kr_0)/kr_0$, integrating with respect to $d(kr_0)$ from zero to infinity and using (3.23), we get

$$-U_0 \sum_{m=0}^{\infty} \epsilon_m i^m \left[\frac{1}{2(m-1)} \delta_{(m-1)s} - \frac{1}{2(m+1)} \delta_{(m+1)s} \right] =$$

$$(i/8) \sum_{n=0}^{\infty} \sum_{m=0}^{\infty} B_n A_{nm} \left[\frac{1}{2(m-1)} \delta_{(m-1)s} - \frac{1}{2(m+1)} \delta_{(m+1)s} \right]$$

Employing the property of kronecker delta, the above equation takes the form

$$-U_0 \left[\epsilon_{s+1} i^{s+1} - \epsilon_{s-1} i^{s-1} \right] =$$

$$(i/8) \left[\sum_{n=0}^{\infty} B_n A_{n(s+1)} - \sum_{n=0}^{\infty} B_n A_{n(s-1)} \right], \quad s = -1, 0, 1, 2, \dots$$

(3.24)

Note that for negative values of the subscripts both ϵ_{s-1} and $A_{n(s-1)}$ are to be taken as zero because those terms correspond to negative values of m in equation (3.22). In equation (3.24) everything is known, except B_n , and this system of equations can easily be solved for the unknowns.

To find the scattered wave for r not on the boundary Γ , equation (2.17) must be used. In two dimensional case we have

$$U^{(s)}(\underline{r}) = \int_{\Gamma} U^{(t)}(\underline{r}_0) \frac{\partial G(\underline{r}, \underline{r}_0)}{\partial n_0} dS_0 \quad (3.25)$$

Using equations (3.3), (3.10), (3.11), (3.13) and (3.14), equation (3.25) becomes

$$U^{(s)}(\underline{r}) = (i/4) \sum_{m=0}^{\infty} H_m^{(1)}(kr) \int_0^{2\pi} \left[\sum_{n=0}^{\infty} B_n \cos n\theta_0 \cos m(\theta - \theta_0) \right. \\ \left. J'_m(kr_0) \frac{ab}{\sqrt{a^2 \sin^2 \theta_0 + b^2 \cos^2 \theta_0}} \right] d\theta_0 \quad (3.26)$$

Using the trigonometric relation (3.16), equation (3.26) takes the form

$$U^{(s)}(\underline{r}) = (i/8) \sum_{m=0}^{\infty} \sum_{n=0}^{\infty} H_m^{(1)}(kr) \cos m\theta B_n \\ \int_0^{2\pi} [\cos(m+n)\theta_0 + \cos(m-n)\theta_0] \frac{J'_m(kr_0) ab d\theta_0}{\sqrt{a^2 \sin^2 \theta_0 + b^2 \cos^2 \theta_0}} \\ + (i/8) \sum_{m=0}^{\infty} \sum_{n=0}^{\infty} H_m^{(1)}(kr) \sin m\theta B_n \\ \int_0^{2\pi} [\sin(m+n)\theta_0 + \sin(m-n)\theta_0] \frac{J'_m(kr_0) ab d\theta_0}{\sqrt{a^2 \sin^2 \theta_0 + b^2 \cos^2 \theta_0}}$$

The above equation is very similar in nature to that given in equation (3.17) and can be written as

$$U^{(s)}(\underline{r}) = (i/8) \sum_{n=0}^{\infty} \sum_{m=0}^{\infty} B_n H_m^{(1)}(kr) \left[A_{nm}^* \cos m\theta + C_{nm}^* \sin m\theta \right] \quad (3.28)$$

where A_{nm}^* and C_{nm}^* have the same form as A_{pm} and C_{pm} given by equation (3.18) except the Hankel functions $H_m^{(1)'}(kr_0)$ in the latter are to be replaced by Bessel functions $J_m'(kr_0)$. By substituting the values of B_n obtained from equation (3.24) the displacement field for any value of r due to the scattered waves can be obtained.

Numerical results for the far field displacements ($r = 2000 r_0$) are presented in Figure 6.

3.2.2 Scattering by a rigid inclusion

In the scattering by a rigid inclusion case, as in the section (3.1.2), the total wave $U^{(t)}$ on the boundary Γ satisfies the integral equation

$$U^{(i)}(\underline{r}) = \int_{\Gamma} G(\underline{r}, \underline{r}_0) \frac{\partial U^{(t)}(\underline{r}_0)}{\partial n_0} dS_0, \quad \underline{r} \text{ on } \Gamma.$$

Using equations (3.1) and (3.6) and going through a similar procedure as explained in the previous section we obtain

$$U^{(i)}(\underline{r}) = (i/4) \sum_{n=0}^{\infty} \sum_{m=0}^{\infty} B_n J_m(kr) \int_0^{2\pi} \left\{ \cos m(\theta - \theta_0) \cos n \theta_0 \right. \\ \left. H_m^{(1)}(kr_0) ab \sqrt{\frac{a^4 \sin^2 \theta_0 + b^4 \cos^2 \theta_0}{(a^2 \sin^2 \theta_0 + b^2 \cos^2 \theta_0)^3}} \right\} d\theta_0$$

(3.29)

Carrying out the integration we get

$$U^{(i)}(\underline{r}) = (i/8) \sum_{n=0}^{\infty} \sum_{m=0}^{\infty} \cos m\theta J_m(kr) B_n D_{nm} + \\ (i/8) \sum_{n=0}^{\infty} \sum_{m=0}^{\infty} \sin m\theta J_m(kr) B_n E_{nm}$$

where

$$D_{nm} = \int_0^{2\pi} \left\{ [\cos(m+n)\theta_0 + \cos(m-n)\theta_0] H_m^{(1)}(kr_0) \right\} ab$$

$$\sqrt{\frac{a^4 \sin^2 \theta_0 + b^4 \cos^2 \theta_0}{(a^2 \sin^2 \theta_0 + b^2 \cos^2 \theta_0)^3}} \Bigg\} d\theta_0$$

(3.30)

$$E_{nm} = \int_0^{2\pi} \left\{ [\sin(m+n)\theta_0 + \sin(m-n)\theta_0] H_m^{(1)}(kr_0) \right\} ab$$

$$\sqrt{\frac{a^4 \sin^2 \theta_0 + b^4 \cos^2 \theta_0}{(a^2 \sin^2 \theta_0 + b^2 \cos^2 \theta_0)^3}} \Bigg\} d\theta_0$$

Recalling the expression for $U^{(i)}(r)$, equation(3.2), the above equation at the boundary becomes

$$U_0 \sum_{m=0}^{\infty} \epsilon_m i^m J_m(kr_0) \cos m\theta_0 =$$

$$(i/8) \sum_{n=0}^{\infty} \sum_{m=0}^{\infty} B_n J_m(kr_0) [D_{nm} \cos m\theta_0 + E_{nm} \sin m\theta_0]$$

To solve for the unknown coefficients B_n , we once again choose $\theta_0 = 0^\circ$ and apply the orthogonality condition as explained in Section (3.2.1), thus we obtain the equation

$$U_0 \epsilon_s i^{s3} = (i/8) \sum_{n=0}^{\infty} B_n D_{ns} \quad , \quad \text{with } s=0,1,2,3,\dots$$

(3.31)

which is analogous to equation (3.24). Equation (3.31) can easily be solved for B_n and together with equation (3.6) they give the $\partial U^{(t)}/\partial n$ at the boundary of the scatterer. In the numerical calculations we have solved for the first ten B_n 's.

Once the value for $\partial U^{(t)}/\partial n$ on the surface is known, using

$$U^{(s)}(\underline{r}) = - \int_{\Gamma} G(\underline{r}, \underline{r}_0) \frac{\partial U^{(t)}(\underline{r}_0)}{\partial n_0} dS_0$$

the scattered wave field for r outside the surface of the scatterer can be obtained. Substituting $G(\underline{r}, \underline{r}_0)$, $\partial U^{(t)}(\underline{r}_0)/\partial n_0$ and dS_0 , one obtains

$$U^{(s)}(\underline{r}) = - (i/4) \sum_{n=0}^{\infty} \sum_{m=0}^{\infty} B_n H_m^{(1)}(kr) \int_0^{2\pi} \left\{ \cos m(\theta - \theta_0) \right. \\ \left. \cos n\theta_0 J_m'(kr_0) ab \sqrt{\frac{a^4 \sin^2 \theta_0 + b^4 \cos^2 \theta_0}{(a^2 \sin^2 \theta_0 + b^2 \cos^2 \theta_0)^3}} \right\} d\theta_0$$

(3.32)

Finally using equation (3.16), equation (3.32) becomes

$$U^{(s)}(\underline{r}) = - (i/8) \sum_{m=0}^{\infty} \sum_{n=0}^{\infty} B_n H_m^{(1)}(kr) \cos m\theta$$

$$\int_0^{2\pi} \left[\cos(m+n)\theta_0 + \cos(m-n)\theta_0 \right] J_m(kr_0) ab$$

$$\left. \sqrt{\frac{a^4 \sin^2 \theta_0 + b^4 \cos^2 \theta_0}{(a^2 \sin^2 \theta_0 + b^2 \cos^2 \theta_0)^3}} \right\} d\theta_0$$

$$- (i/8) \sum_{m=0}^{\infty} \sum_{n=0}^{\infty} B_n H_m^{(1)}(kr) \sin m\theta$$

$$\int_0^{2\pi} \left[\sin(m+n)\theta_0 + \sin(m-n)\theta_0 \right] J_m(kr_0) ab$$

$$\left. \sqrt{\frac{a^4 \sin^2 \theta_0 + b^4 \cos^2 \theta_0}{(a^2 \sin^2 \theta_0 + b^2 \cos^2 \theta_0)^3}} \right\} d\theta_0$$

(3.33)

The above equation can be written as a sum of two terms

$$U^{(s)}(\underline{r}) = - (i/8) \sum_{n=0}^{\infty} \sum_{m=0}^{\infty} B_n H_m^{(1)}(kr) \left[D_{nm}^* \cos m\theta + E_{nm}^* \sin m\theta \right]$$

(3.34)

where D_{nm}^* and E_{nm}^* have the same form as D_{nm} and E_{nm} given by equation (3.30) except the Hankel functions $H_m^{(1)}(kr_0)$ in the latter are to be replaced by Bessel functions $J_m(kr_0)$. By substituting the values of B_n obtained from equation (3.31) the displacement field for any value of r due to the scattered waves can be obtained.

Numerical results for the far-field displacements ($r = 2000 r_0$) are presented in Figure 7.

CHAPTER IV

DISCUSSION AND CONCLUSION

This work's goal is the integral formulation of the field equations of elasticity theory in an attempt to analyse the scattering phenomenon of SH-waves from circular and elliptical cavities and rigid inclusions. To this end the governing differential equation is transformed into an integral equation and solved by the Hilbert-Schmidt method. This method is first applied to the scattering of SH-waves by a circular cavity and rigid inclusion. It is known that the Hilbert-Schmidt method is applicable only when the kernel of the integral equation can be represented by a series of orthogonal functions suitable for the geometry of the scatterer. In the case of a circular cylinder, the orthogonal functions are the Bessel functions and using orthogonality conditions, this problem is solved exactly. However, the result being in the form of an infinite series, should be truncated at some point to make it suitable for numerical computation. To this aim only the first ten expressions are used, and the results for near- and far-field displacements with near-field stress distributions are obtained. The graphs corresponding to these solutions are found to be almost exact.

Then the Hilbert-Schmidt theory is used to solve the scattering problem by elliptical cylinder. Basically, the diffraction of waves by an elliptic cylinder is not much different from the diffraction caused by a circular

cylinder. There is of course no difficulty in setting up the appropriate integral equations for a particular problem, the difficulty lies in solving them. In mathematical analysis, because of the geometry of the scatterer, an entirely different wave function must be used, involving products of Mathieu functions.

Since Bessel functions are easier to handle and more suitable to numerical computation, Bessel functions are used instead of Mathieu for the scattering problem by an elliptical cylinder and this choice aside from the elliptical case, allows one to deal other shapes much more efficiently.

On the other hand, the use of Bessel functions instead of Mathieu makes it impossible to benefit from the orthogonality conditions and the resulting integrals are solved numerically. Again only the first ten expressions of the infinite series are used to plot the near- and far-field displacements. Since far-field solutions converge much more faster than that of the near-field, only excellent results for this case could be obtained. Also the graphs representing far-field solutions of the scattered wave are found to be in fair agreement for up to $k \leq 1$, whereas for $k > 1$ the solutions roughly resemble those of the exact solution. This is also due to the fact that, the series with increasing wave number, loses its asymptotic character, though it is still convergent.

RESULTS

FIGURE CAPTIONS

- Figure 1 Displacement at the boundary of a circular cavity, due to the scattered wave field.
- (a) $ka = 0.1$
 - (b) $ka = 0.5$
 - (c) $ka = 1.0$
 - (d) $ka = 10.0$
- Figure 2 Far-field displacement due to the scattered wave field from a circular cavity.
- (a) $ka = 0.1$
 - (b) $ka = 0.5$
 - (c) $ka = 1.0$
 - (d) $ka = 5.0$
 - (e) $ka = 10.0$
- Figure 3 Tangential stresses $\left| \partial U^{(s)} / \partial \theta \right|$ on the boundary of a circular cavity due to the scattered wave field.
- (a) $ka = 0.1$
 - (b) $ka = 0.5$
 - (c) $ka = 1.0$
 - (d) $ka = 10.0$
- Figure 4 Far-field displacement due to the scattered wave field from a rigid circular inclusion.
- (a) $ka = 0.1$
 - (b) $ka = 0.5$
 - (c) $ka = 1.0$
 - (d) $ka = 5.0$

Figure 5 Normal stress $|\partial U^{(s)} / \partial r|$ on the boundary of a rigid circular inclusion due to the scattered wave field.

(a) $ka = 0.1$

(b) $ka = 0.5$

(c) $ka = 1.0$

Figure 6 Far-field displacement due to the scattered wave field from an elliptical cavity.

(a) $k=0.1$, $a=1.0$, $b=0.5$

(b) $k=0.1$, $a=0.5$, $b=1.0$

(c) $k=0.5$, $a=1.0$, $b=0.5$

(d) $k=0.5$, $a=0.5$, $b=1.0$

(e) $k=1.0$, $a=1.0$, $b=0.5$

(f) $k=1.0$, $a=0.5$, $b=1.0$

(g) $k=5.0$, $a=1.0$, $b=0.5$

(h) $k=5.0$, $a=0.5$, $b=1.0$

(i) $k=5.0$, $a=0.5$, $b=2.5$

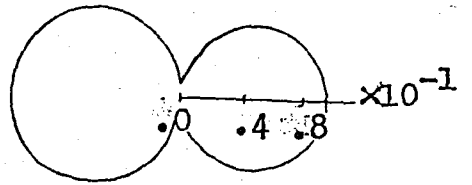
Figure 7 Far-field displacement due to the scattered wave field from a rigid elliptical inclusion.

(a) $k=1.0$, $a=1.0$, $b=0.5$

(b) $k=1.0$, $a=0.5$, $b=1.0$

(c) $k=5.0$, $a=1.0$, $b=0.5$

(d) $k=5.0$, $a=0.5$, $b=1.0$



Exact solution [15]

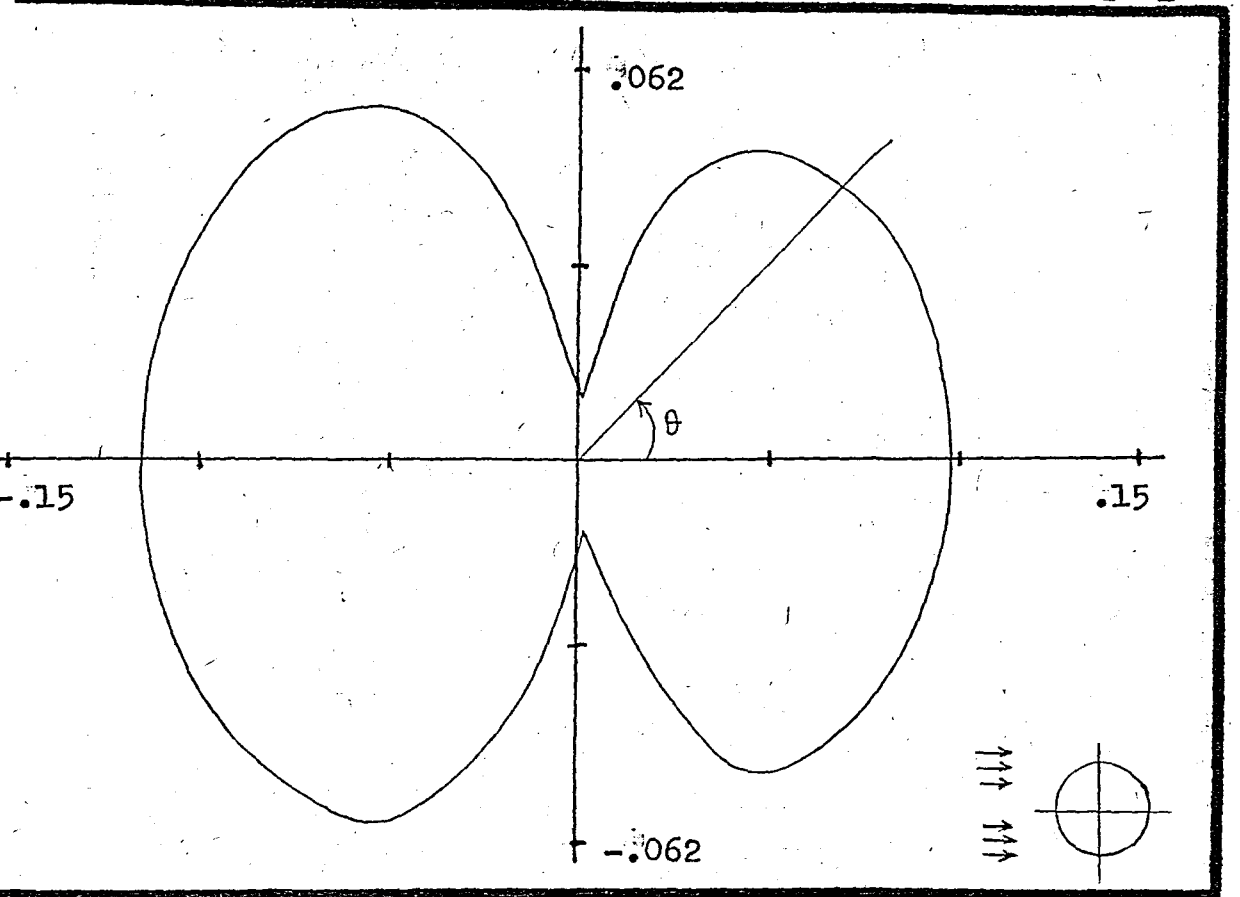
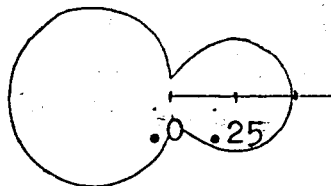


Figure 1: Displacement at the boundary of a circular cavity, due to the scattered wave field.

1(a) $ka = 0.1$



Exact solution [15]

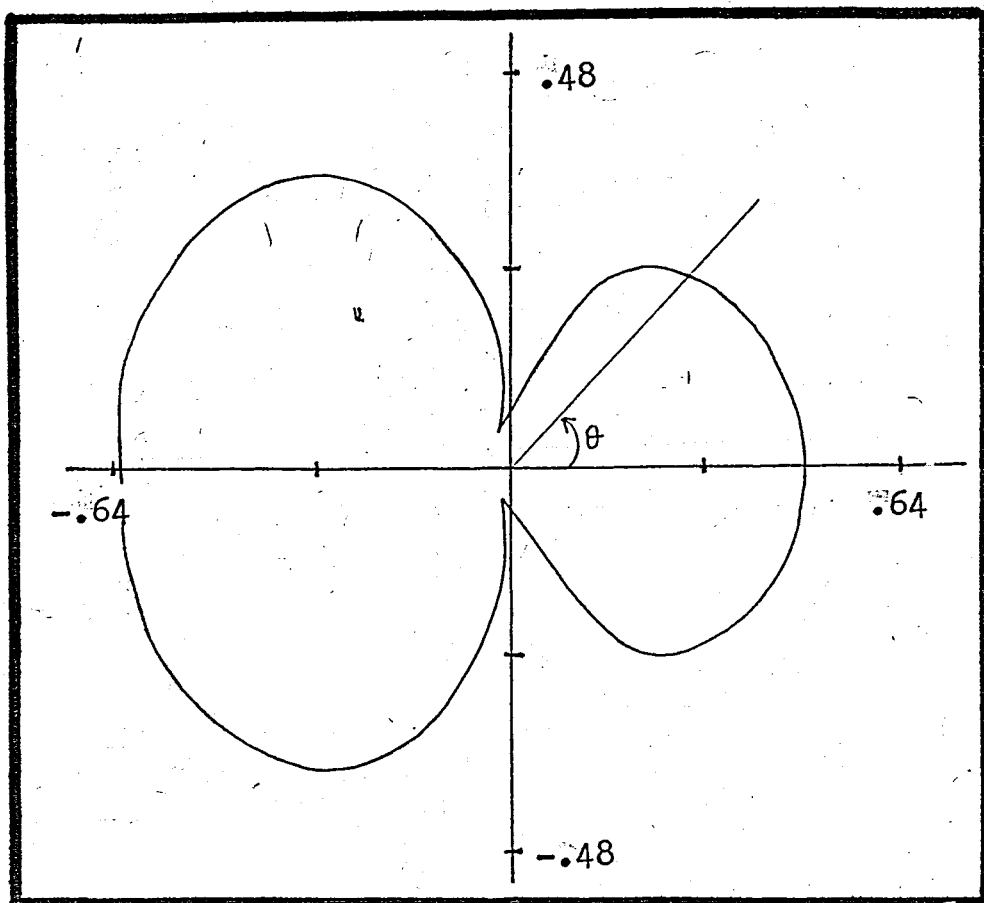
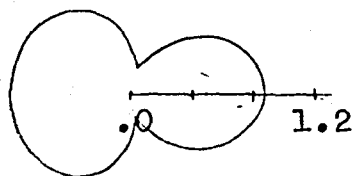
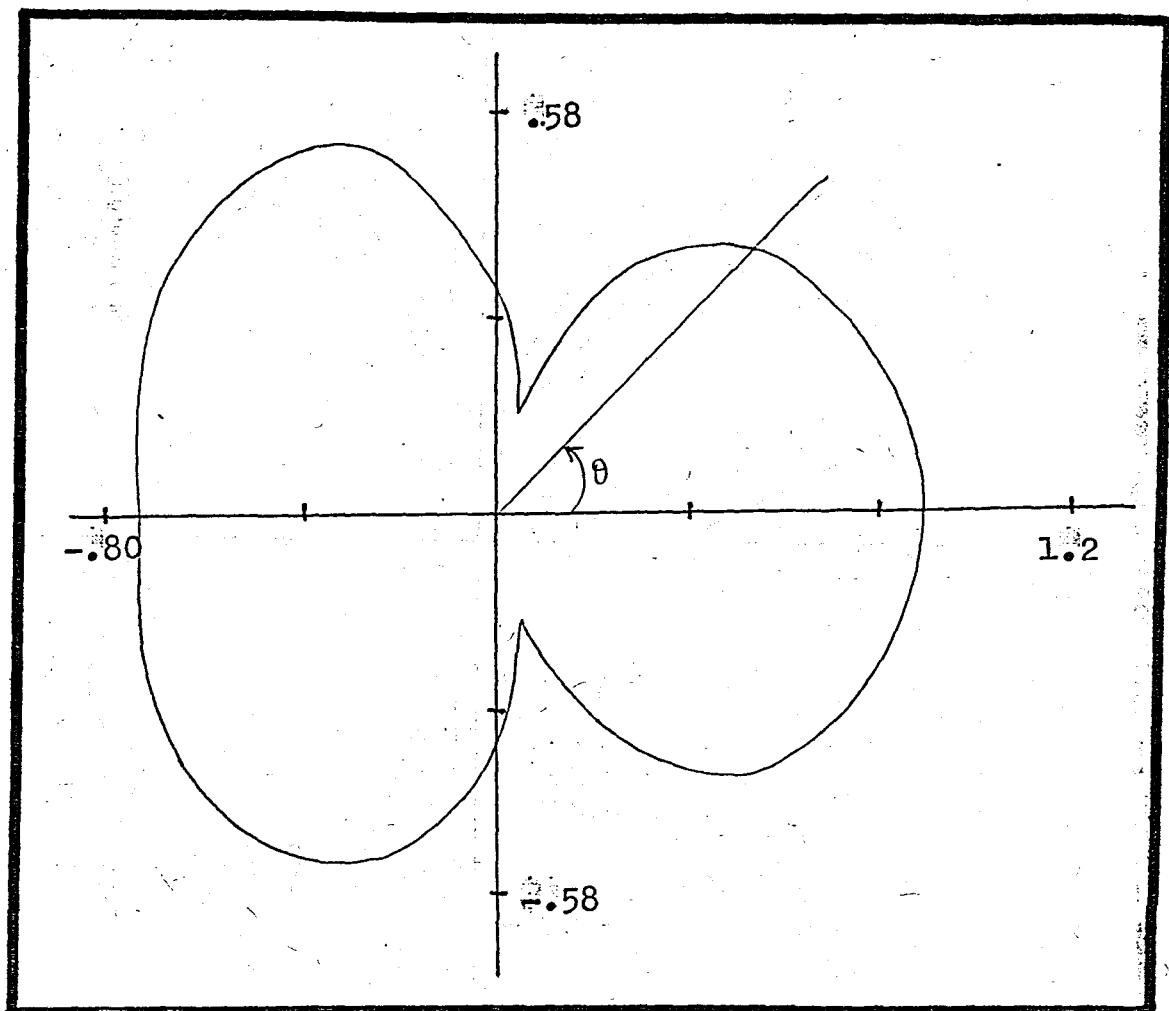


Figure 1(b) $ka=0.5$



Exact Solution [15]

Figure 1(c) $ka = 1.0$

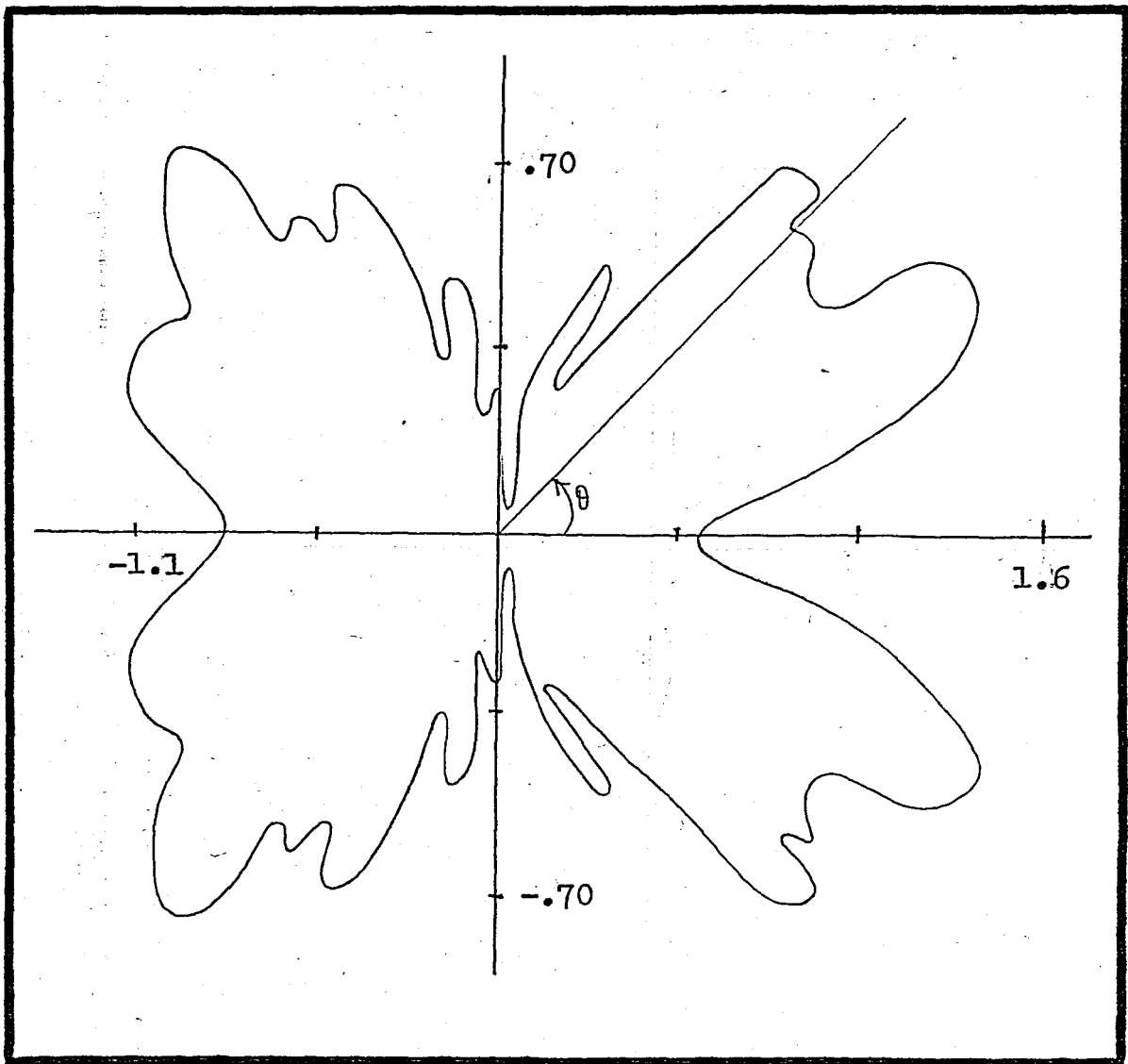
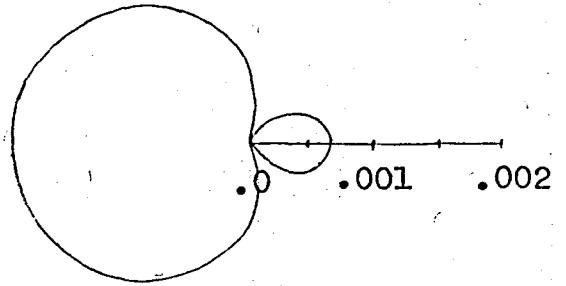


Figure 1(d) $ka = 10.0$



Exact solution [15]^(*)

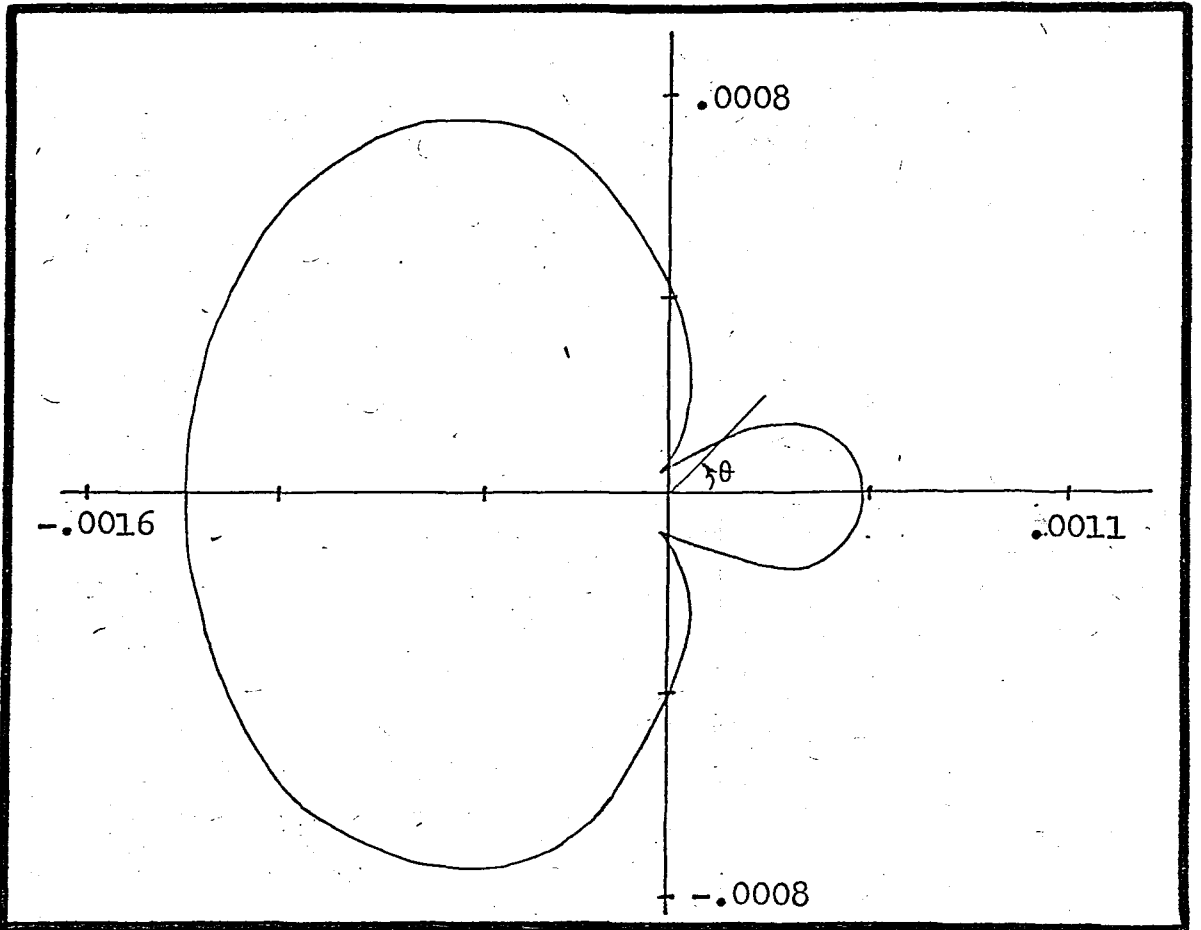
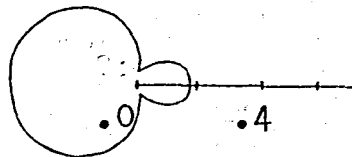


Figure 2 Far-field displacement due to the scattered wave field from a circular cavity.

2(a) $ka = 0.1$

(*) This figure is a polar plot of $\lim_{r \rightarrow \infty} \left| \frac{\sqrt{kr} U^{(s)}}{e^{ikr}} \right|$



Exact solution [15]^(*)

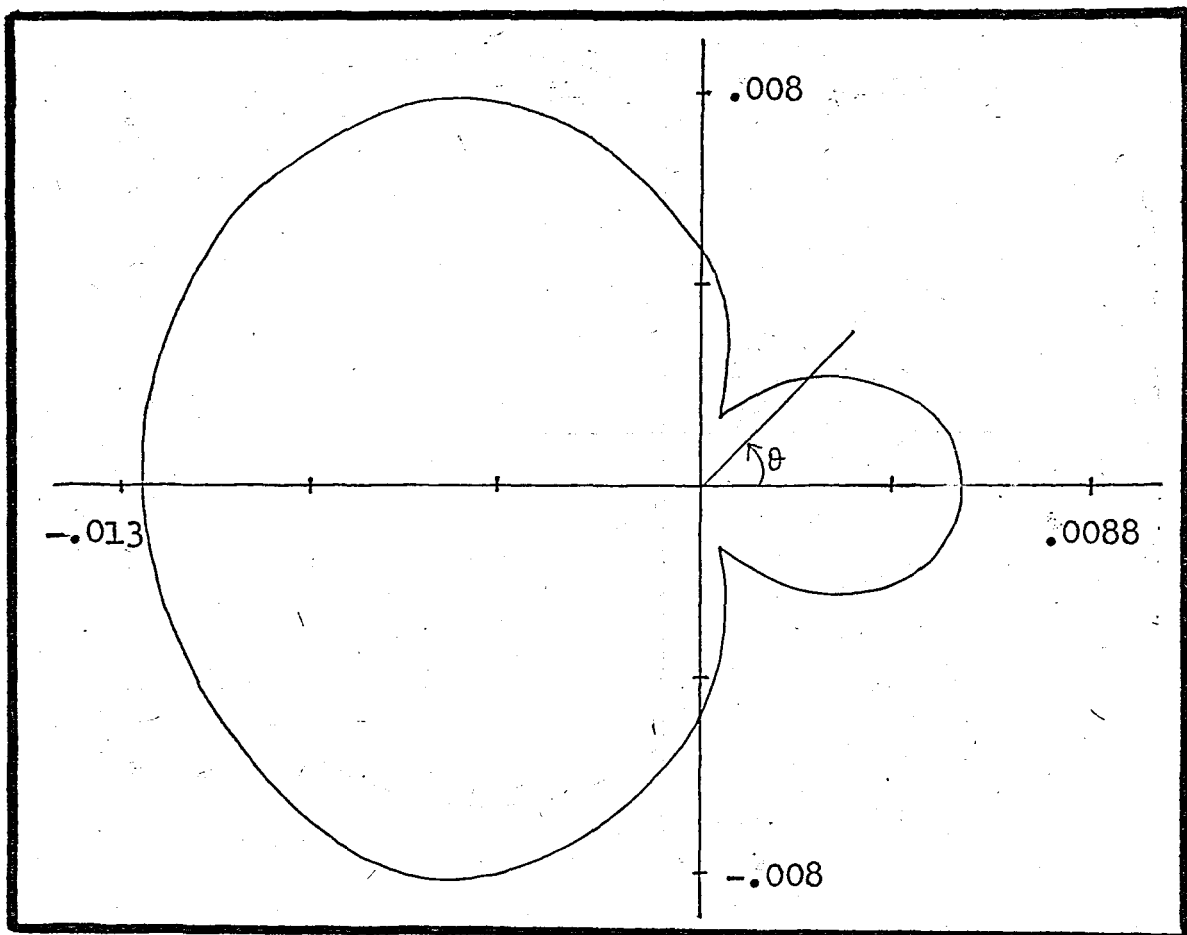
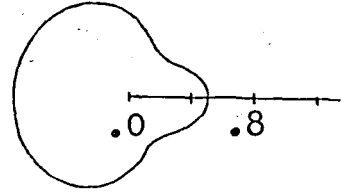


Figure 2(b) $ka = 0.5$

(*) This figure is a polar plot of $\lim_{r \rightarrow \infty} \left| \frac{\sqrt{kr} U(s)}{e^{ikr}} \right|$



Exact solution [15]^(*)

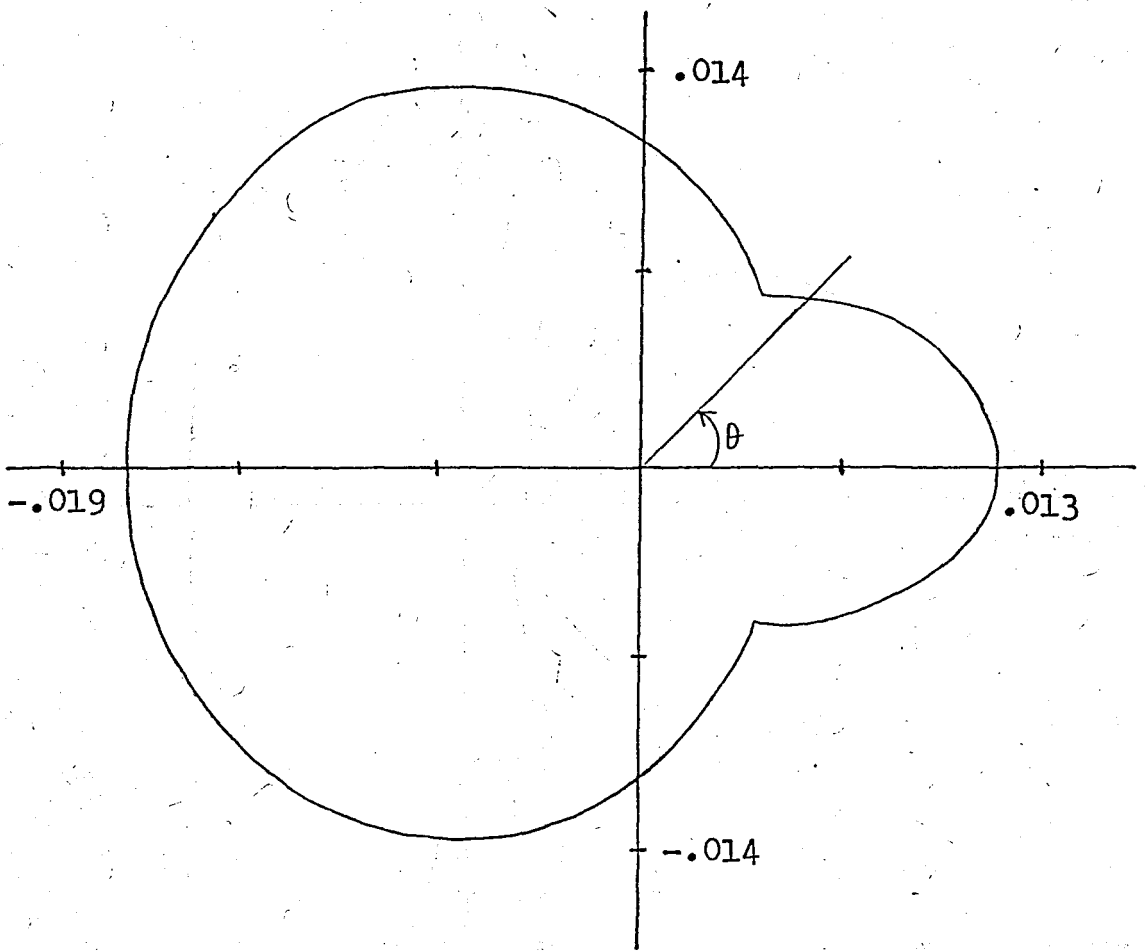


Figure 2(c) $ka = 1.0$

(*) This figure is a polar plot of $\lim_{r \rightarrow \infty} \left| \frac{\sqrt{kr} U^{(s)}}{e^{ikr}} \right|$

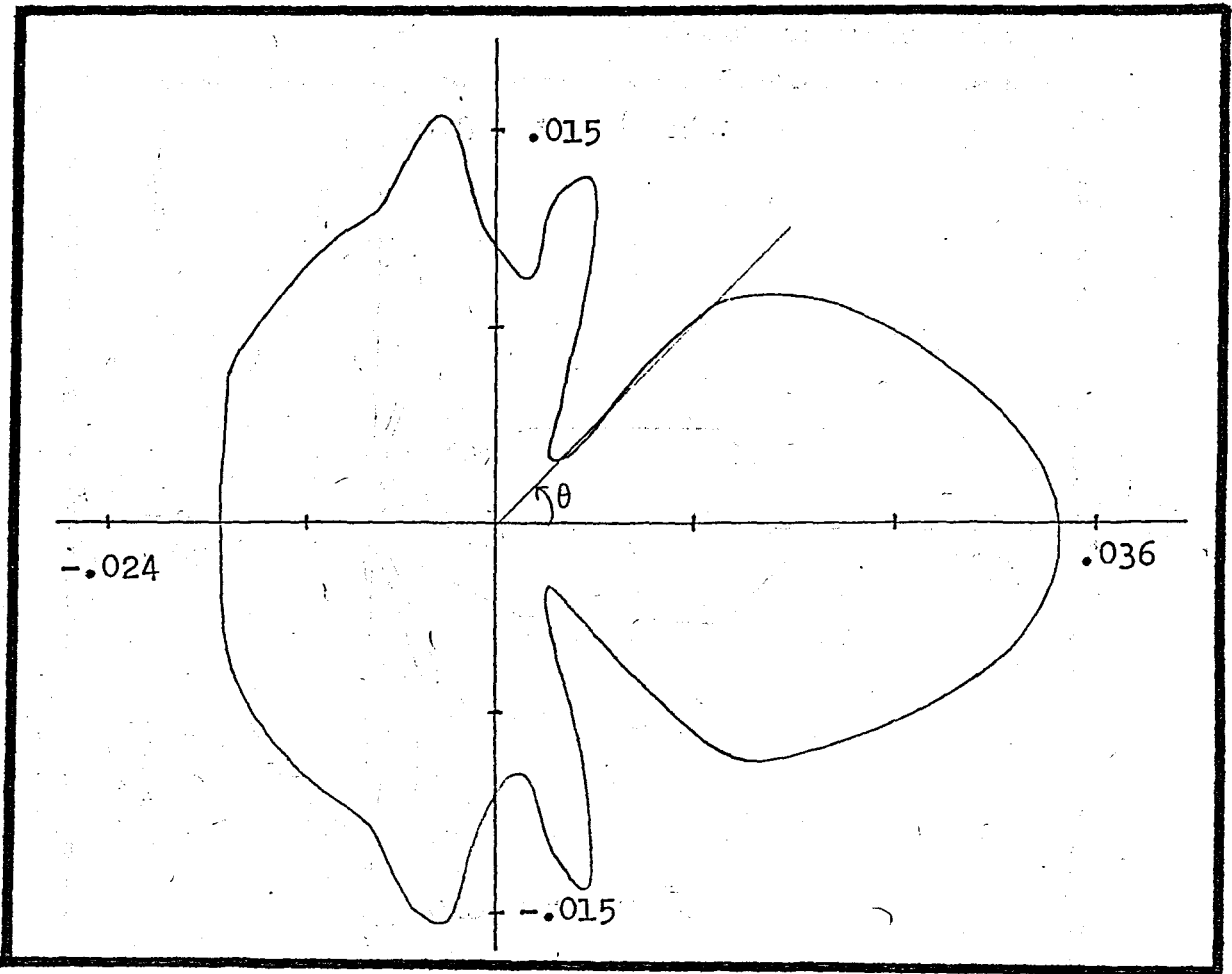
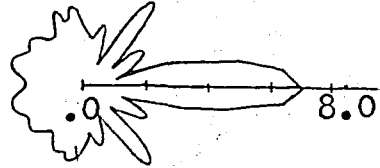


Figure 2(d) $ka = 5.0$



Exact solution [15]^(*)

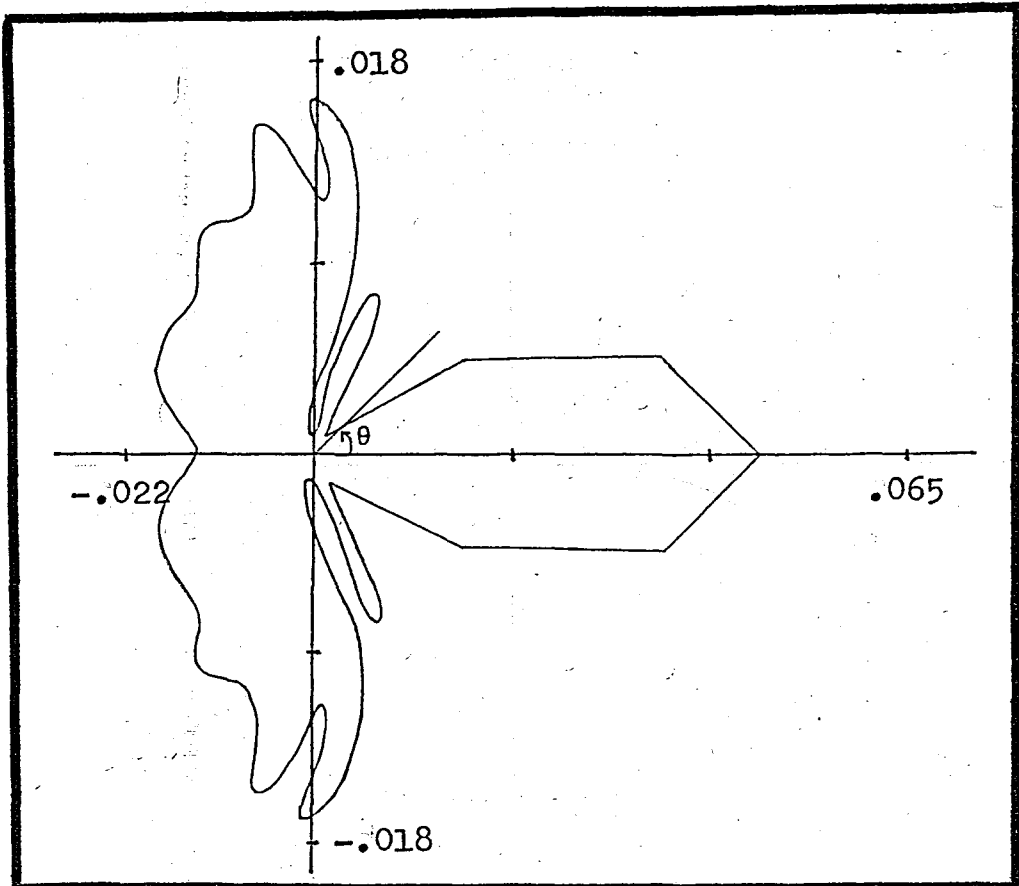
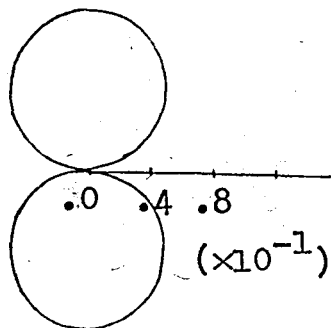


Figure 2(e) $ka = 10.0$

(*) This figure is a polar plot of $\lim_{r \rightarrow \infty} \left| \frac{\sqrt{kr} U(s)}{e^{ikr}} \right|$



Exact solution [15]

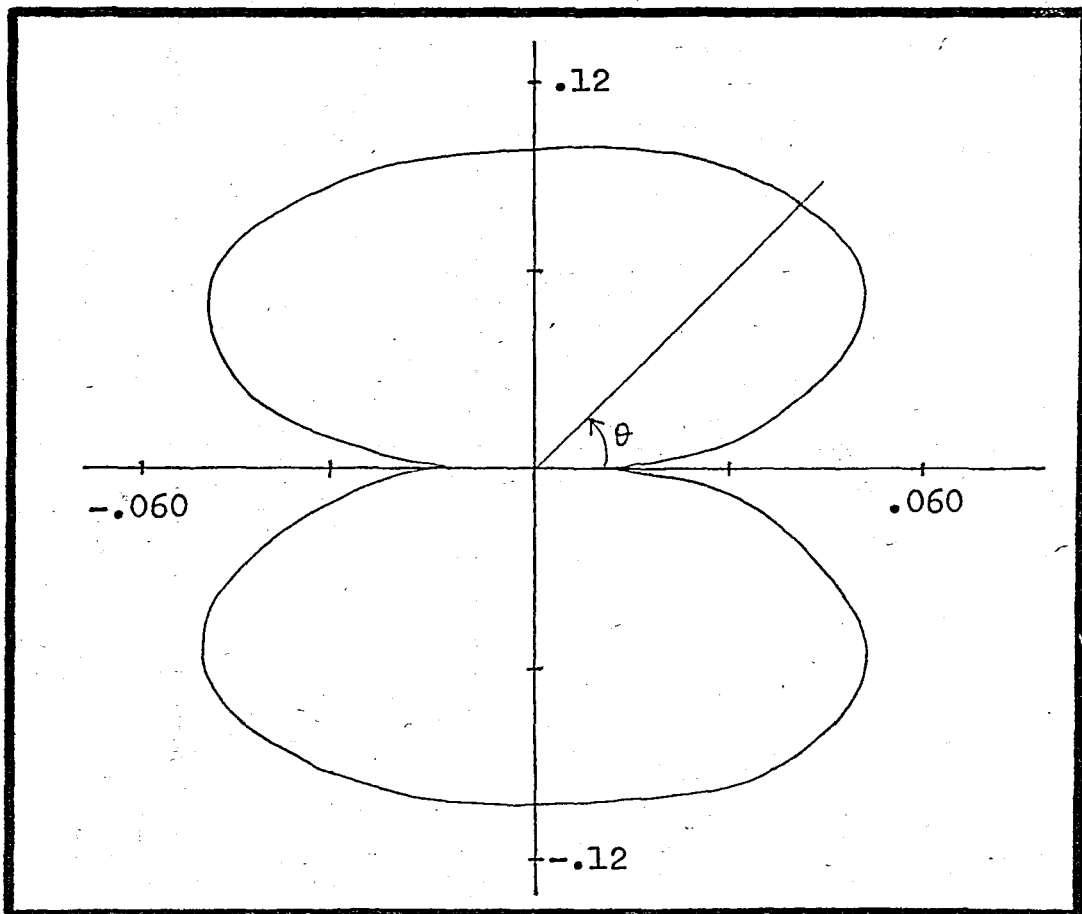
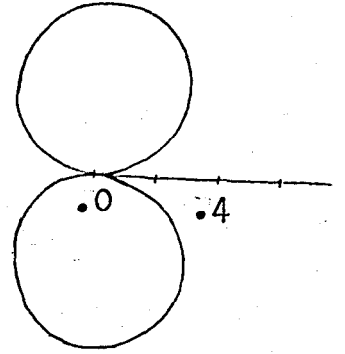


Figure 3 Tangential stress $|\partial U^{(s)} / \partial \theta|$ on the boundary of a circular cavity due to the scattered wave field.

3(a) $ka = 0.1$



Exact solution [15]

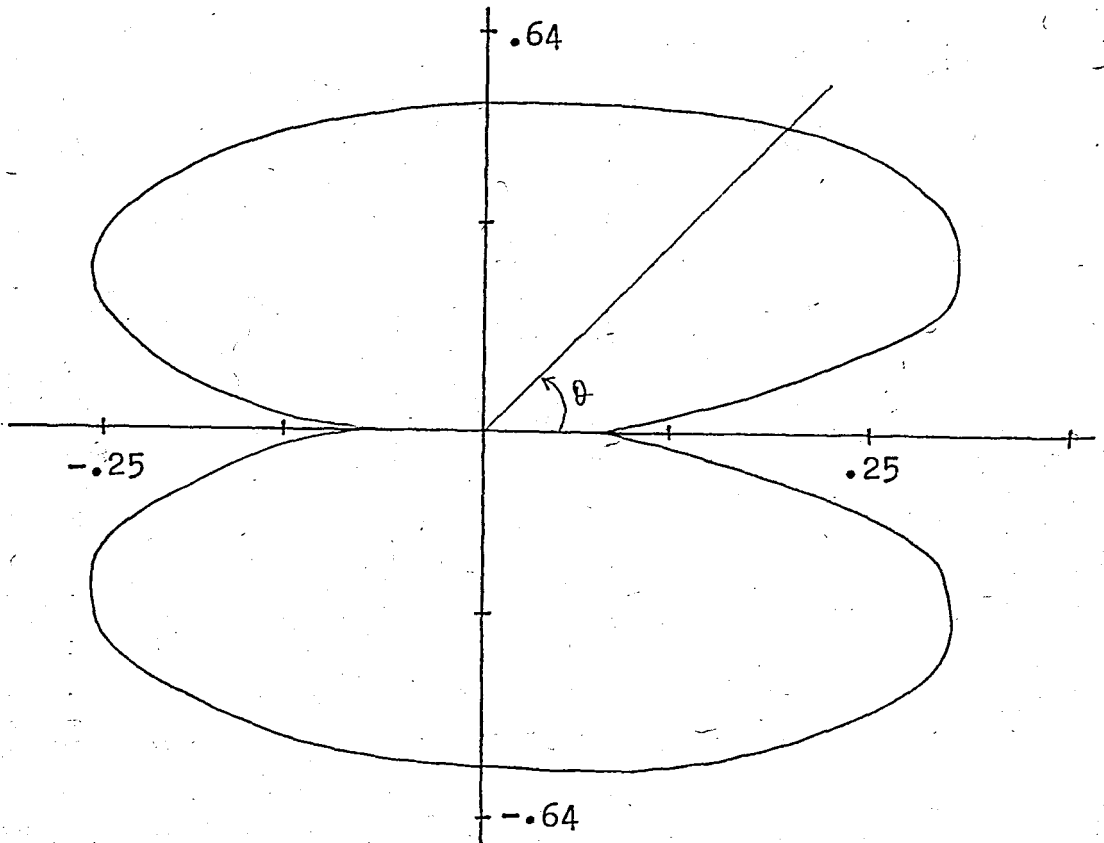
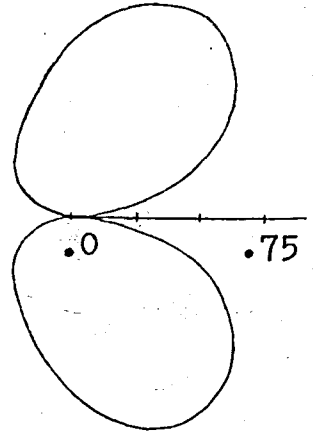


Figure 3(b) $ka = 0.5$



Exact solution [15]

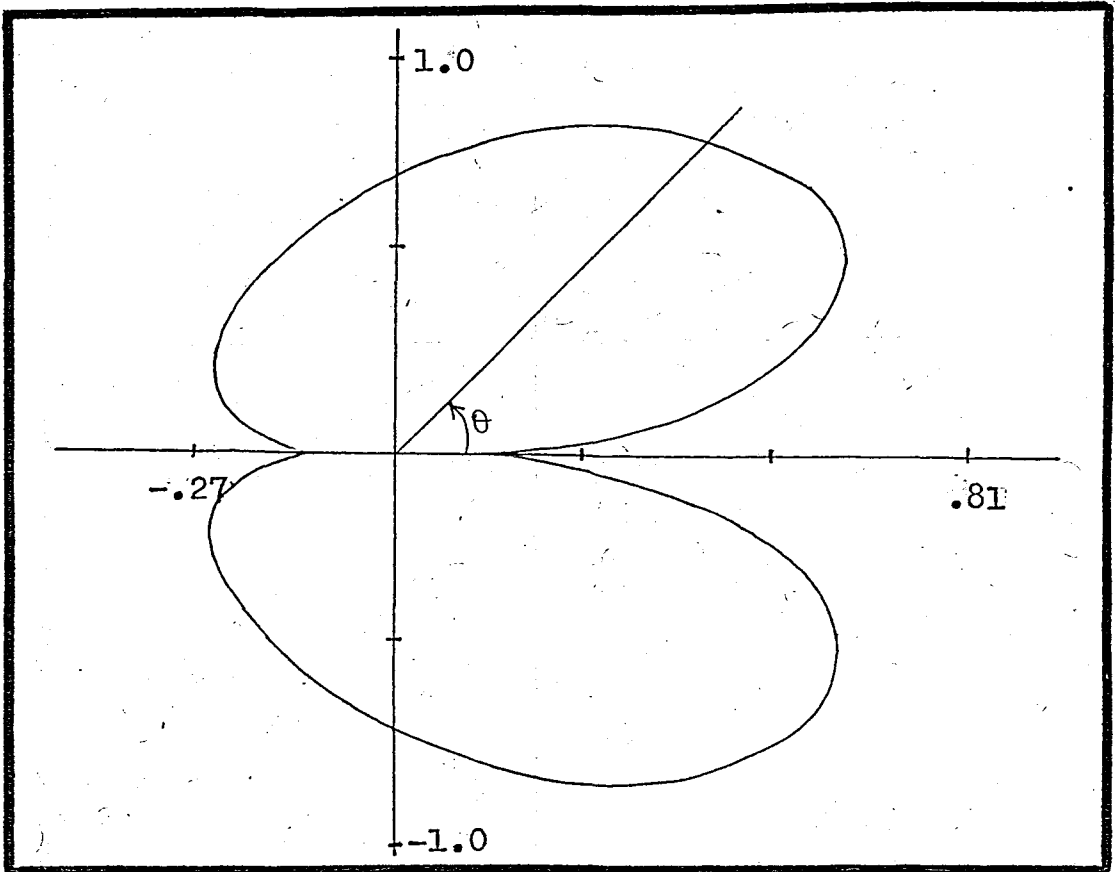


Figure 3(c) $ka = 1.0$

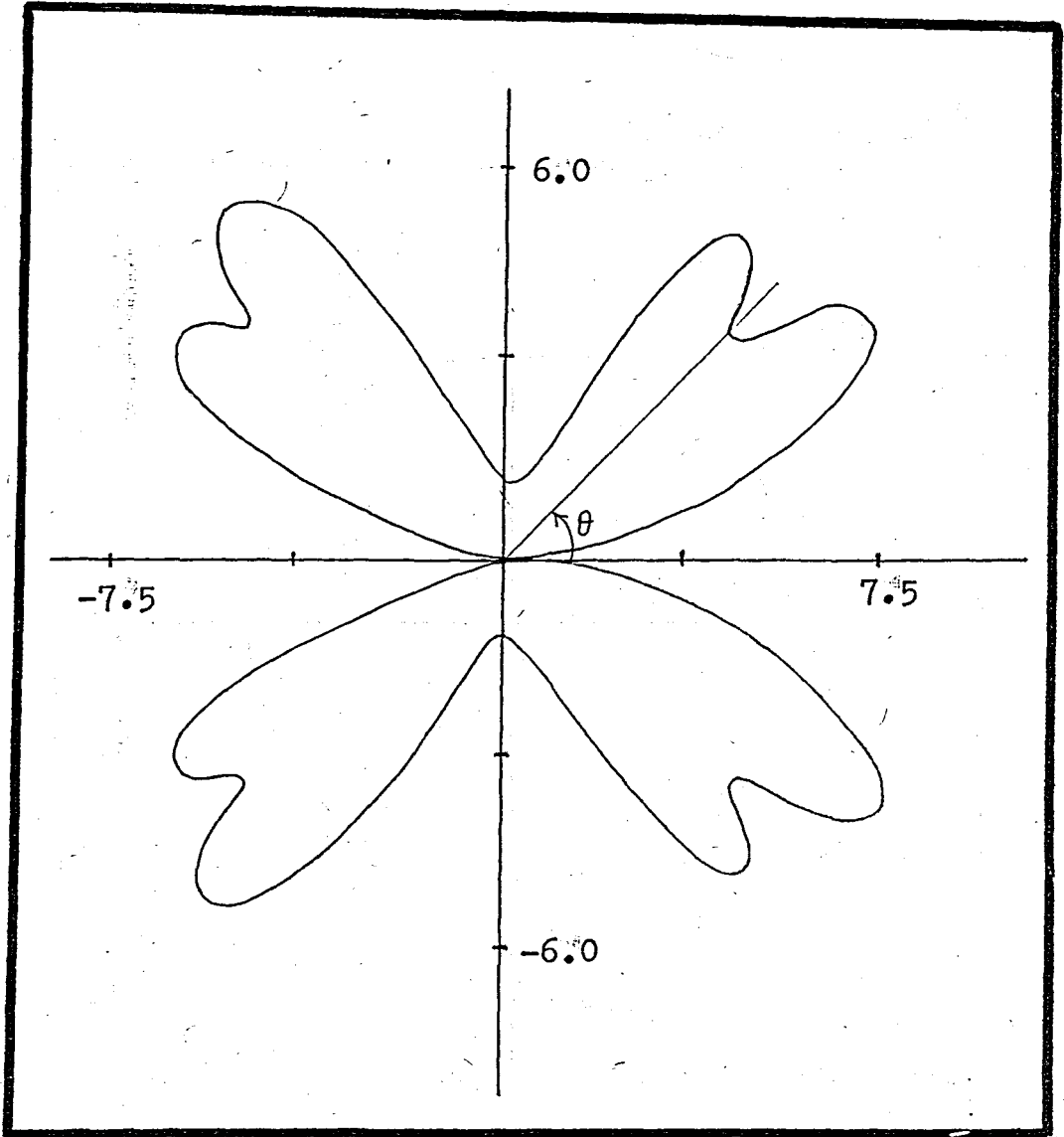
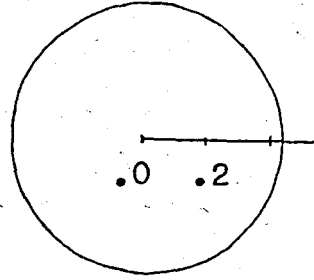


Figure 3(d) $ka = 10.0$



Exact solution [15]^(*)

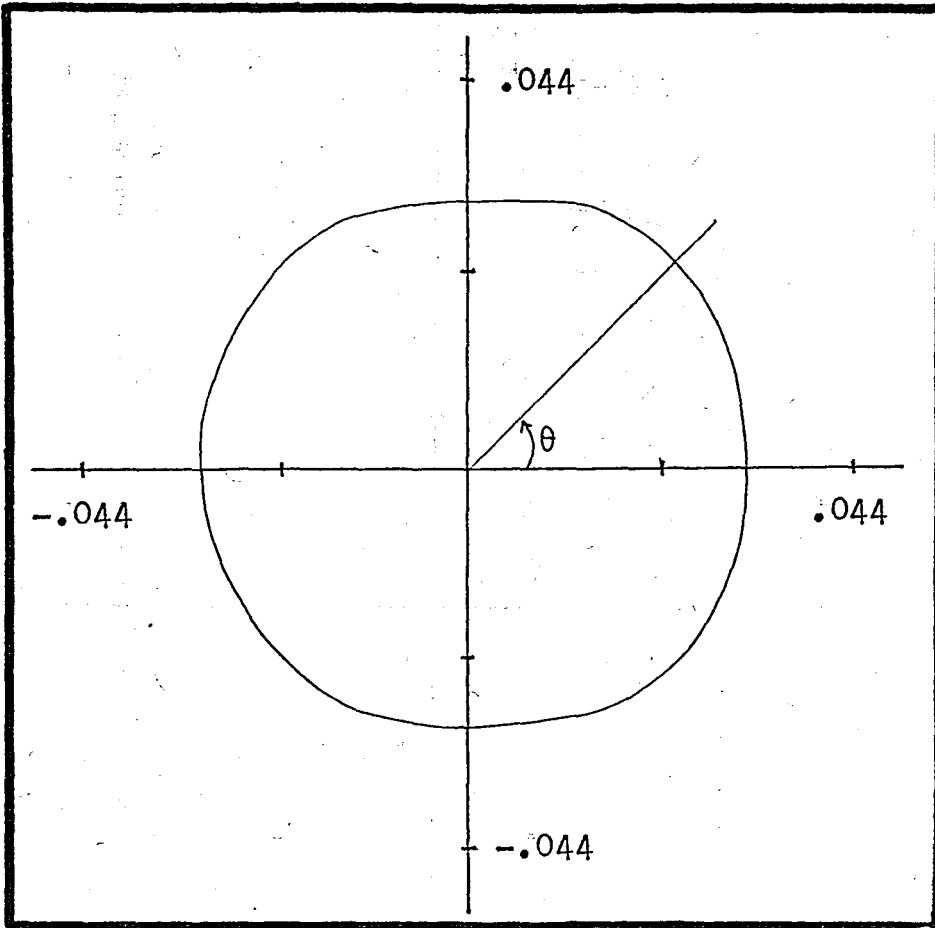
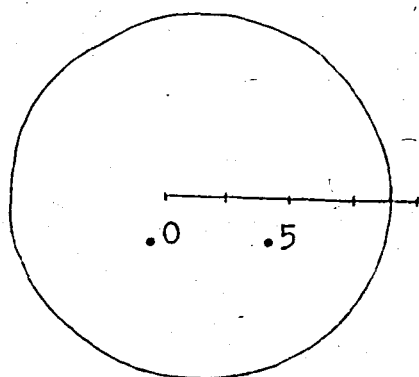


Figure 4 Far-field displacement due to the scattered wave field from a rigid circular inclusion.

4(a) $ka = 0.1$

(*) This figure is a polar plot of $\lim_{r \rightarrow \infty} \left| \frac{\sqrt{kr} U^{(s)}}{e^{ikr}} \right|$



Exact solution [15]^(*)

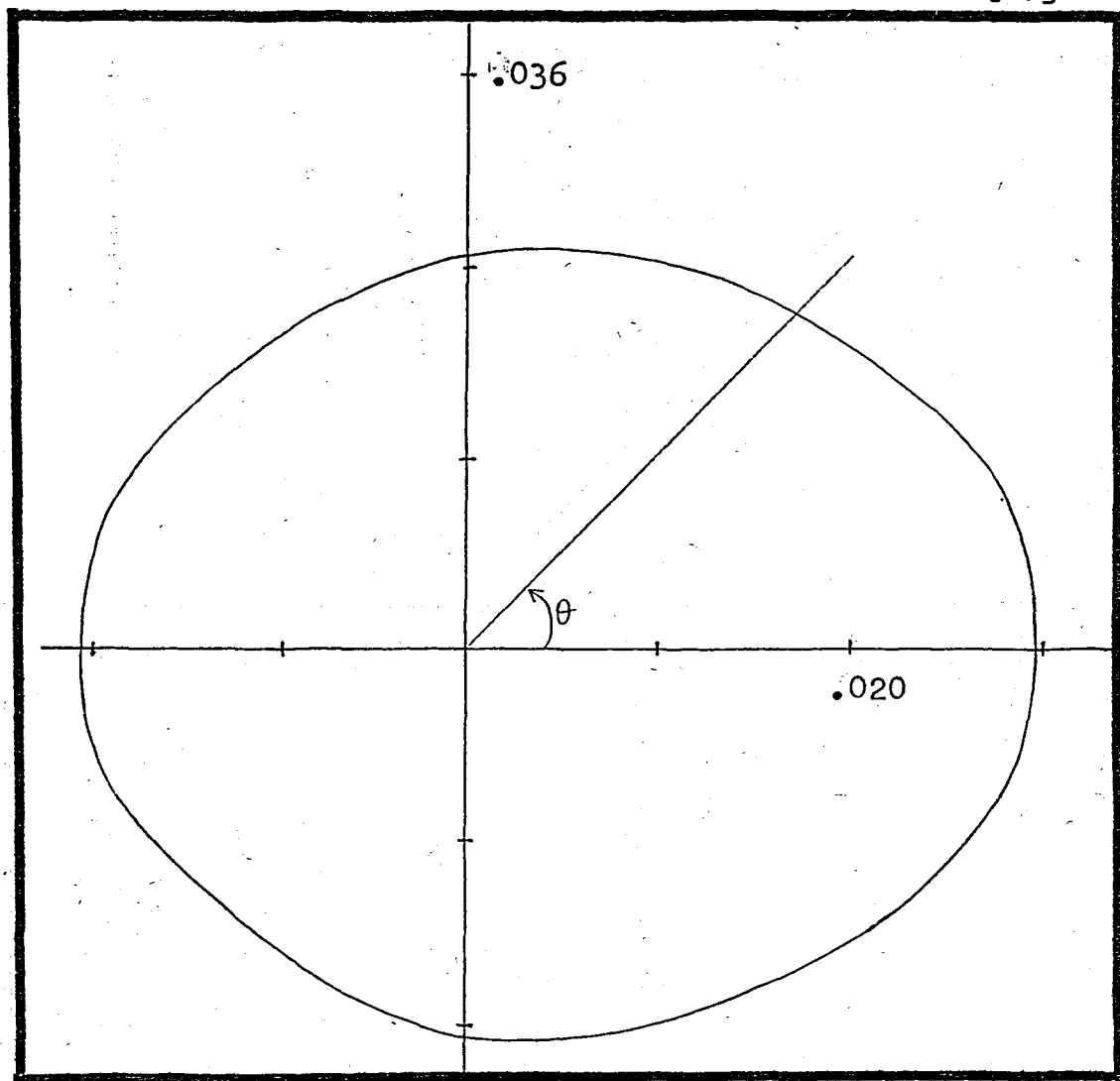
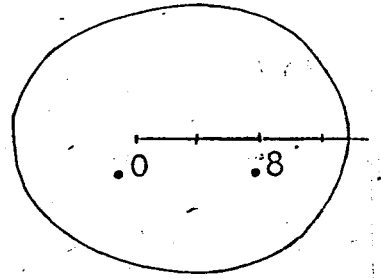


Figure 4(b) $ka = 0.5$

(*) This figure is a polar plot of $\lim_{r \rightarrow \infty} \left| \frac{\sqrt{kr} U(s)}{e^{ikr}} \right|$



Exact solution [15] (*)

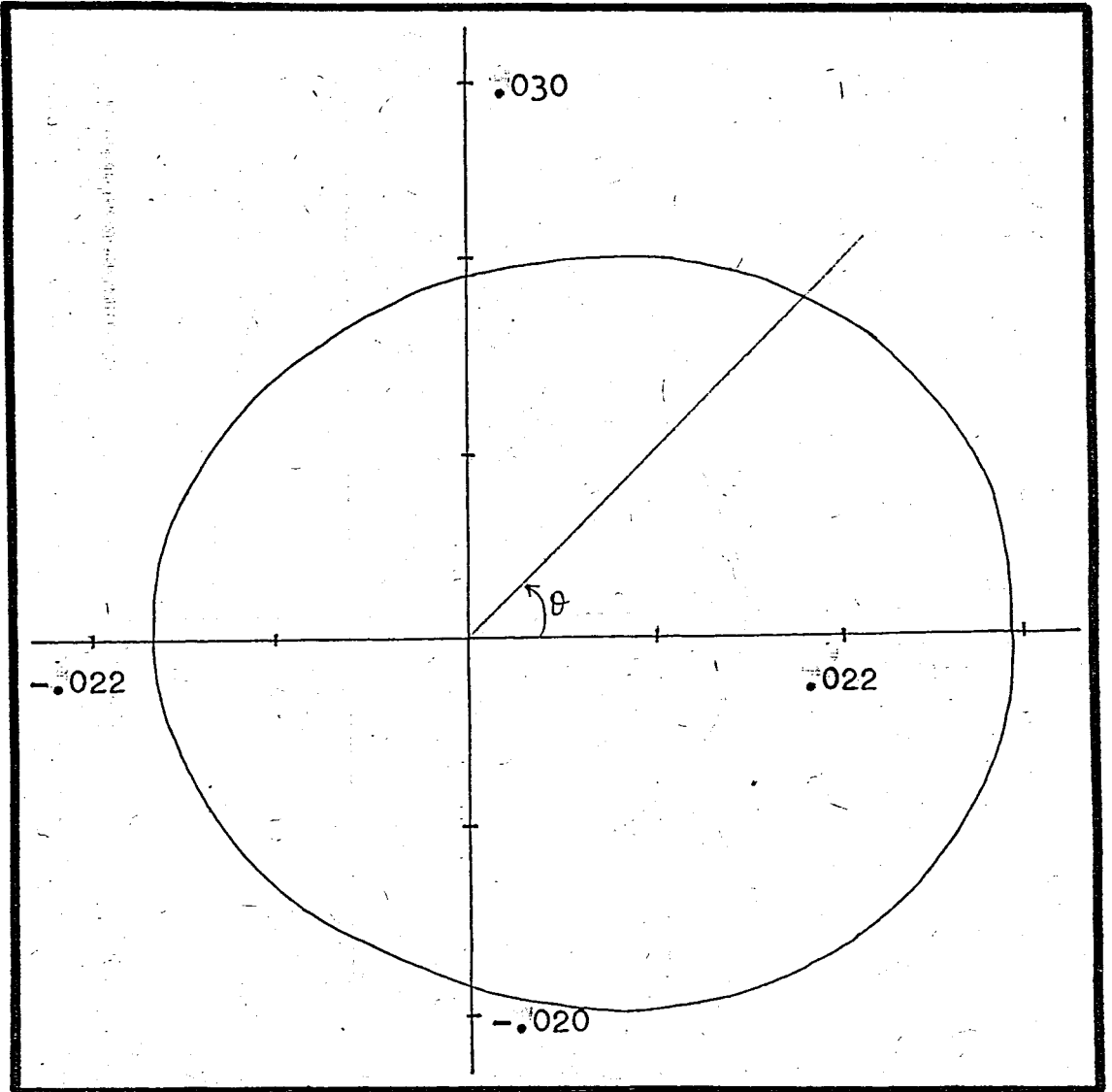


Figure 4(c) $ka = 1.0$

(*) This figure is a polar plot of $\lim_{r \rightarrow \infty} \left| \frac{\sqrt{kr} U(s)}{e^{ikr}} \right|$

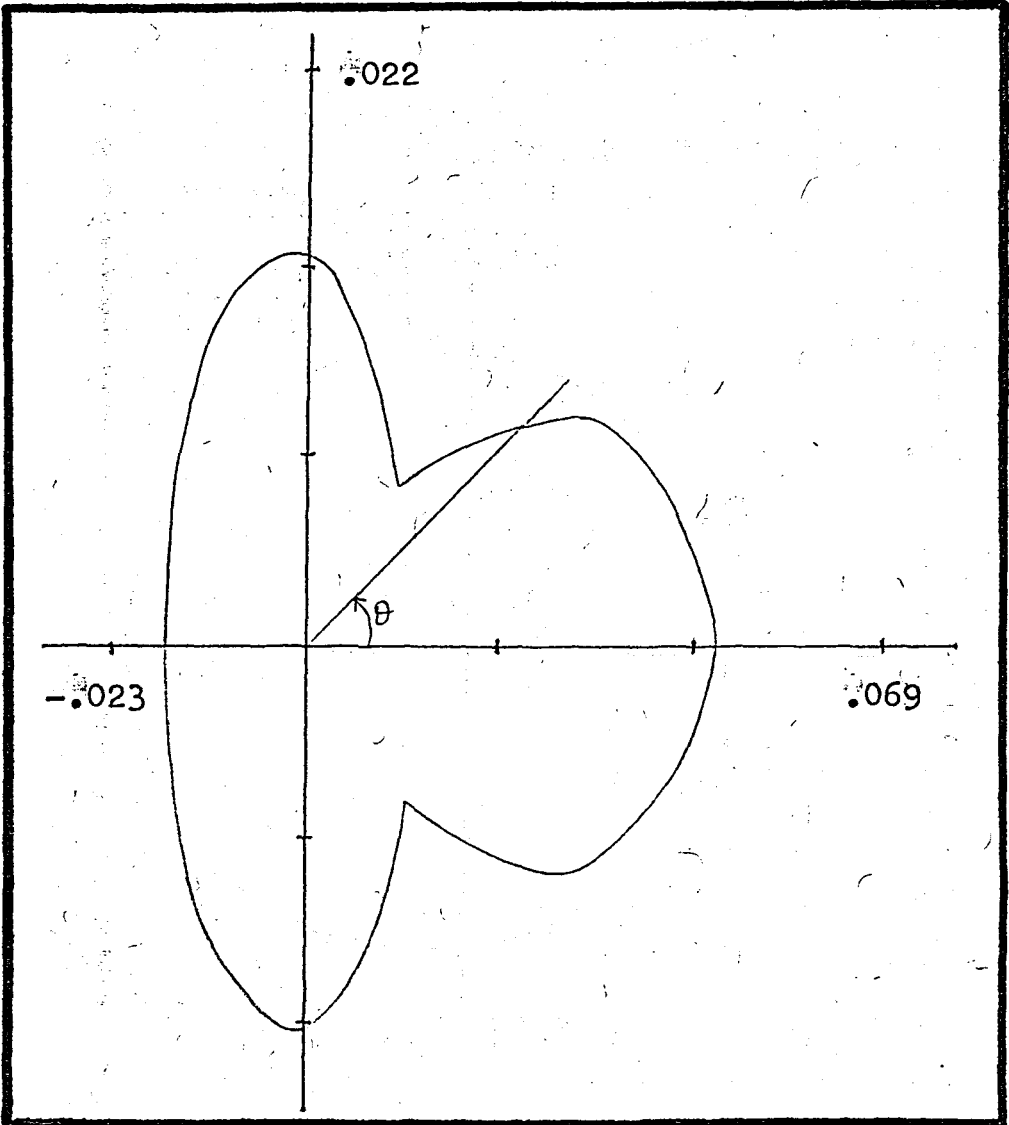
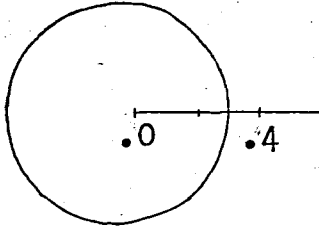


Figure 4(d) $ka = 5.0$



Exact solution [15]

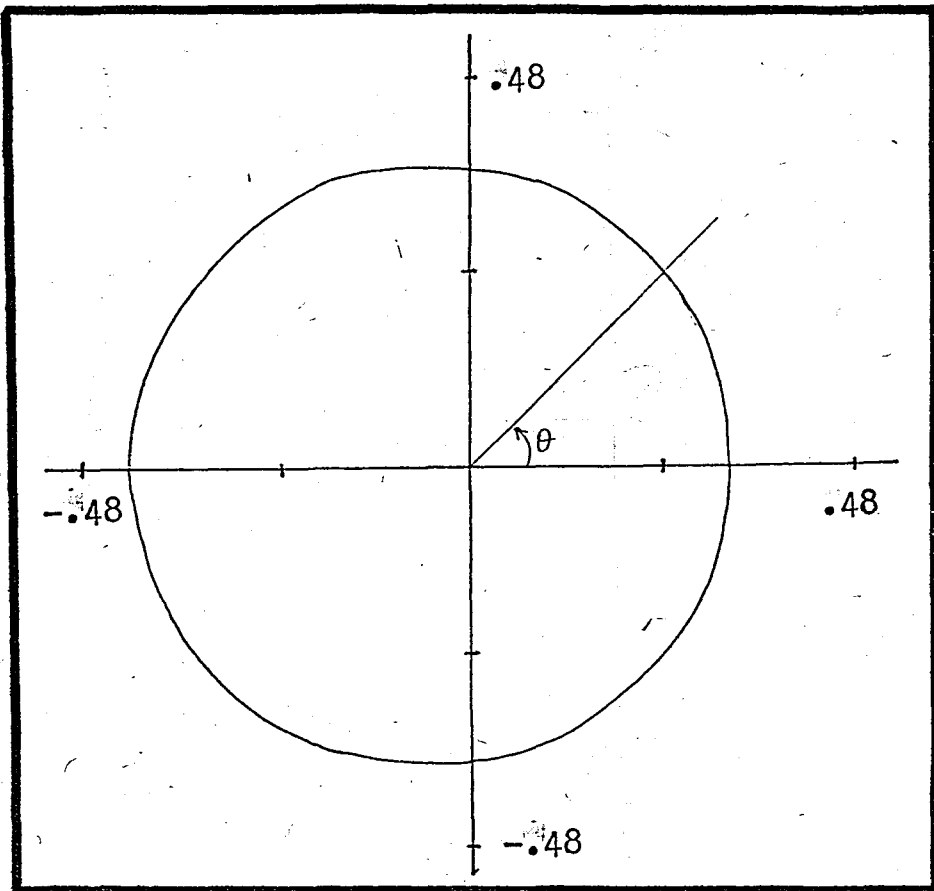
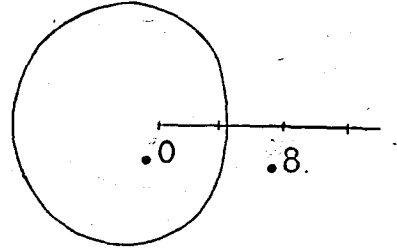
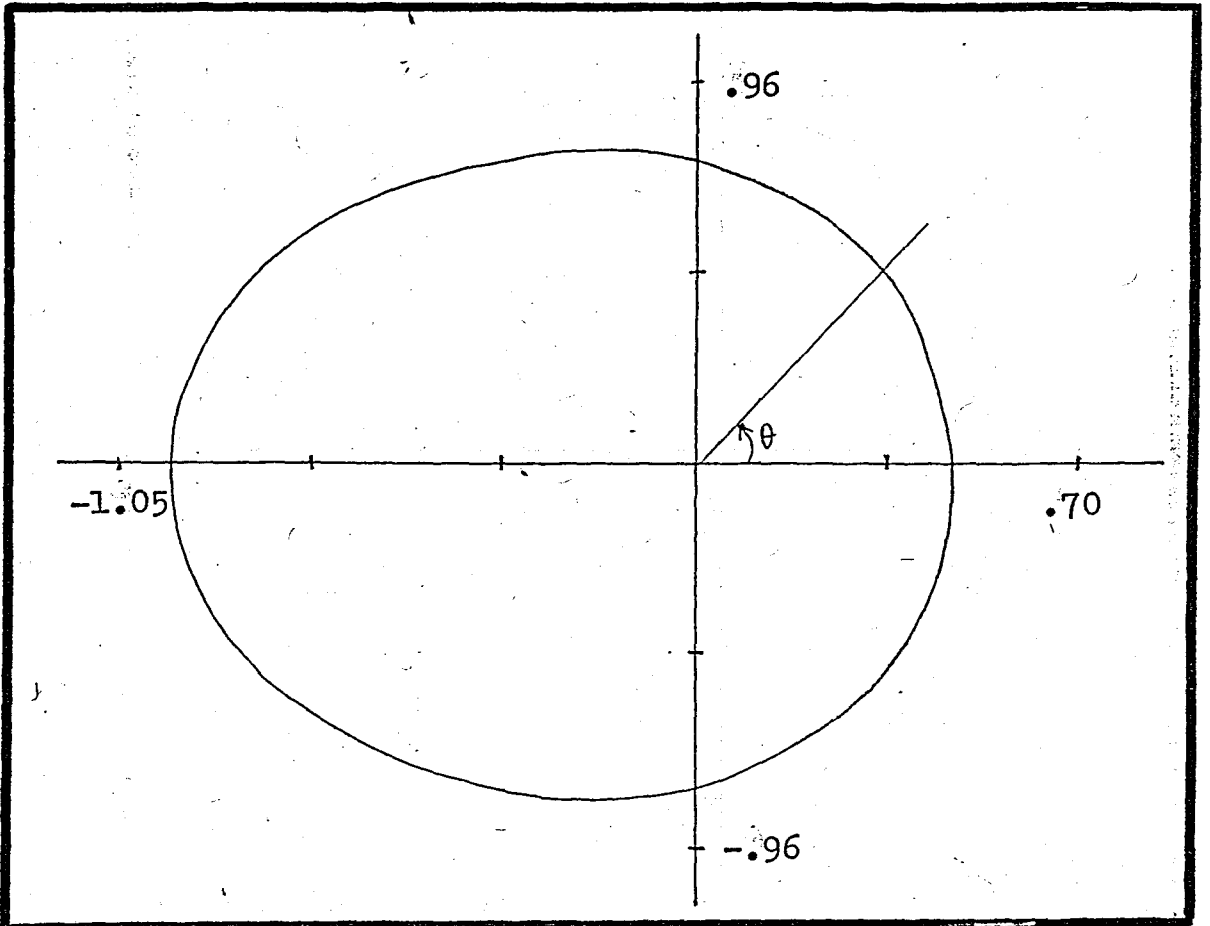


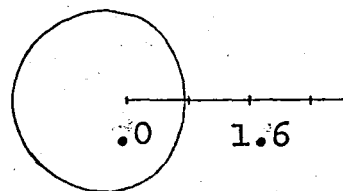
Figure 5 Normal stress $|\partial U^{(s)} / \partial r|$ on the boundary of a rigid circular inclusion due to the scattered wave field.

5(a) $ka = 0.1$

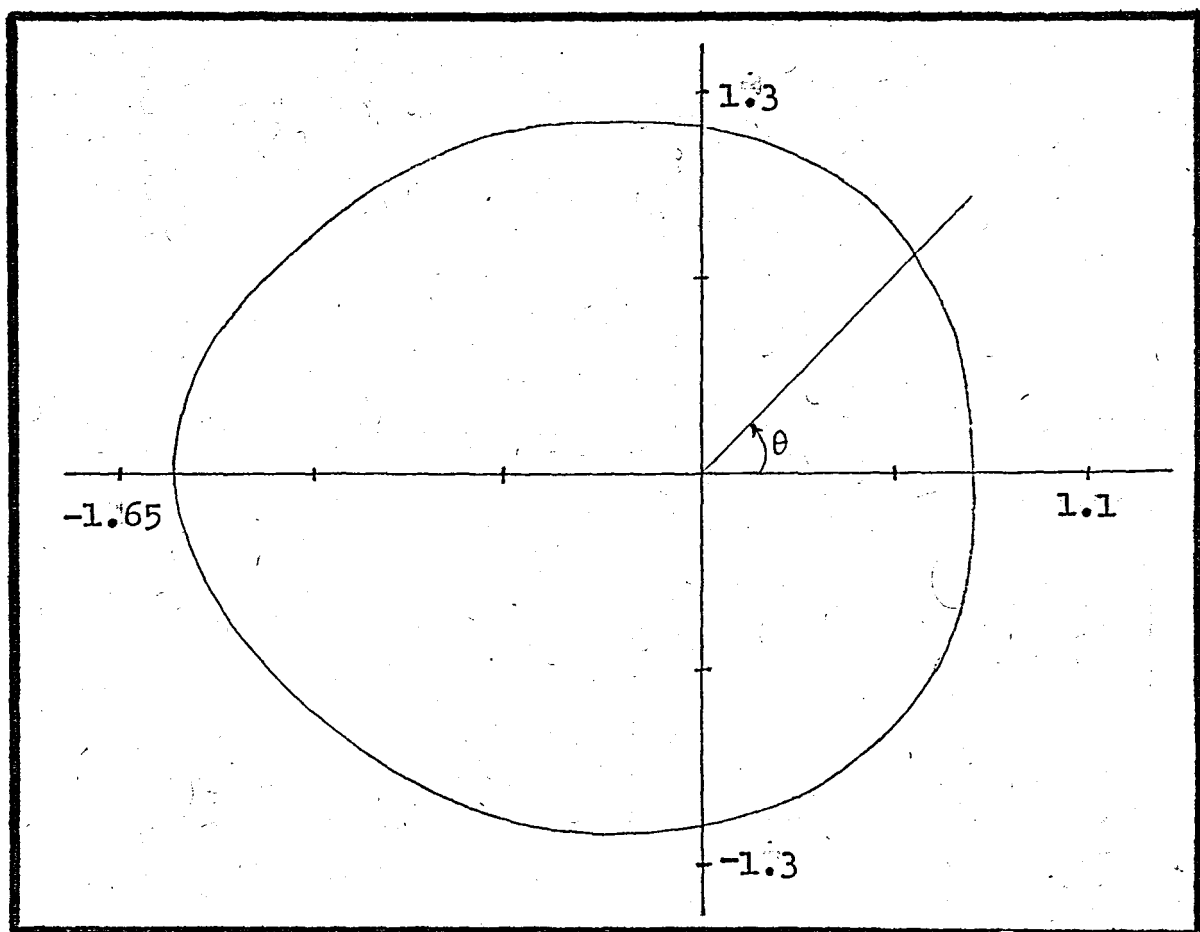


Exact solution [15]

Figure 5(b) $ka = 0.5$



Exact solution [15]

Figure 5(c) $ka = 1.0$

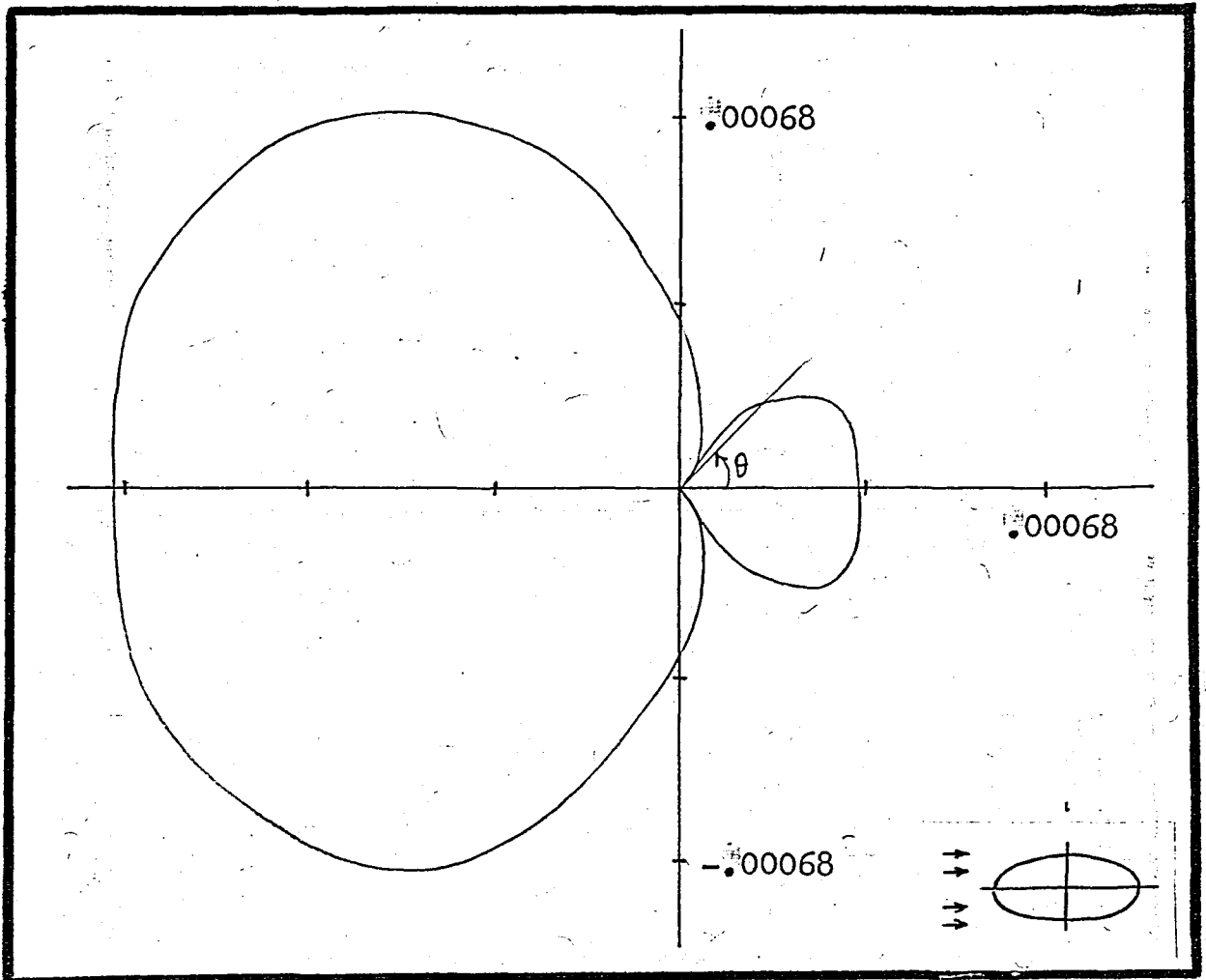


Figure 6 Far-field displacement due to the scattered wave field from an elliptical cavity.

6(a) $k=0.1$, $a=1.0$, $b=0.5$

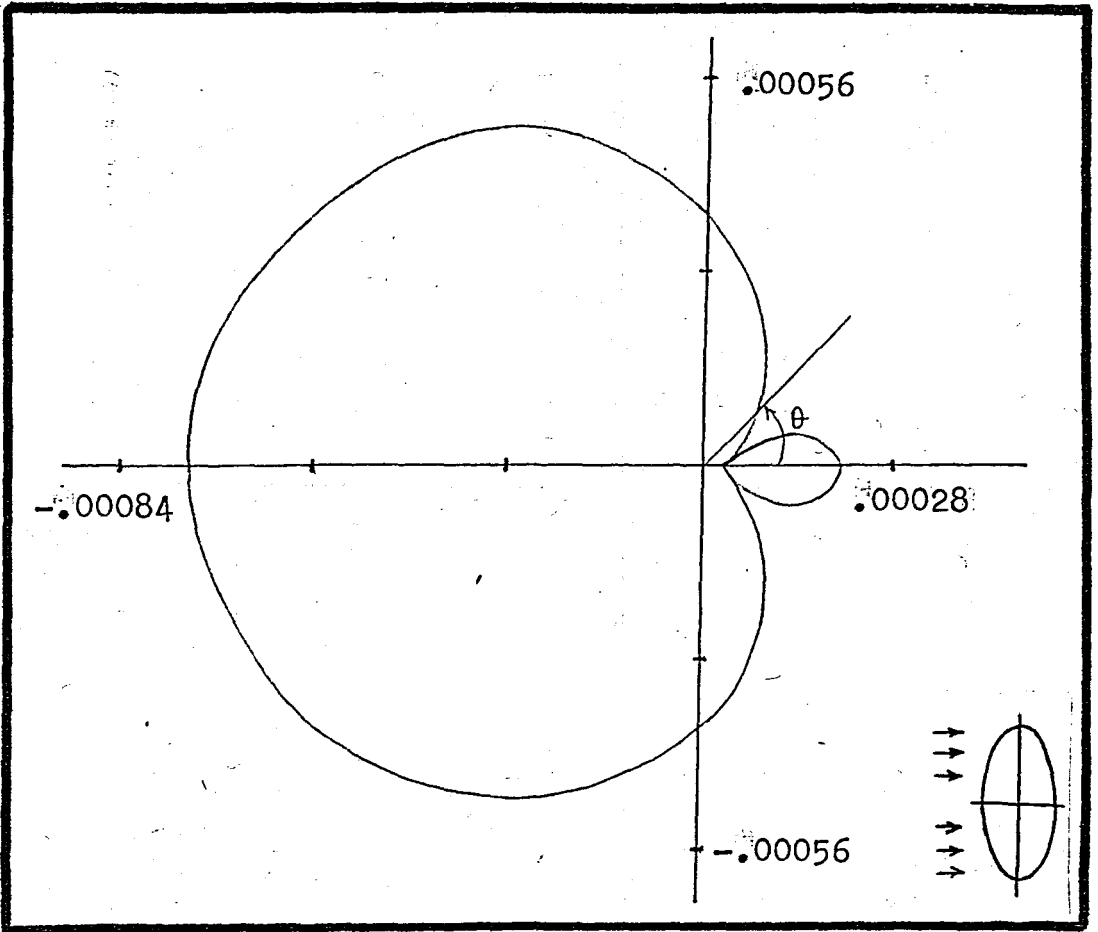


Figure 6(b) $k=0.1$, $a=0.5$, $b=1.0$

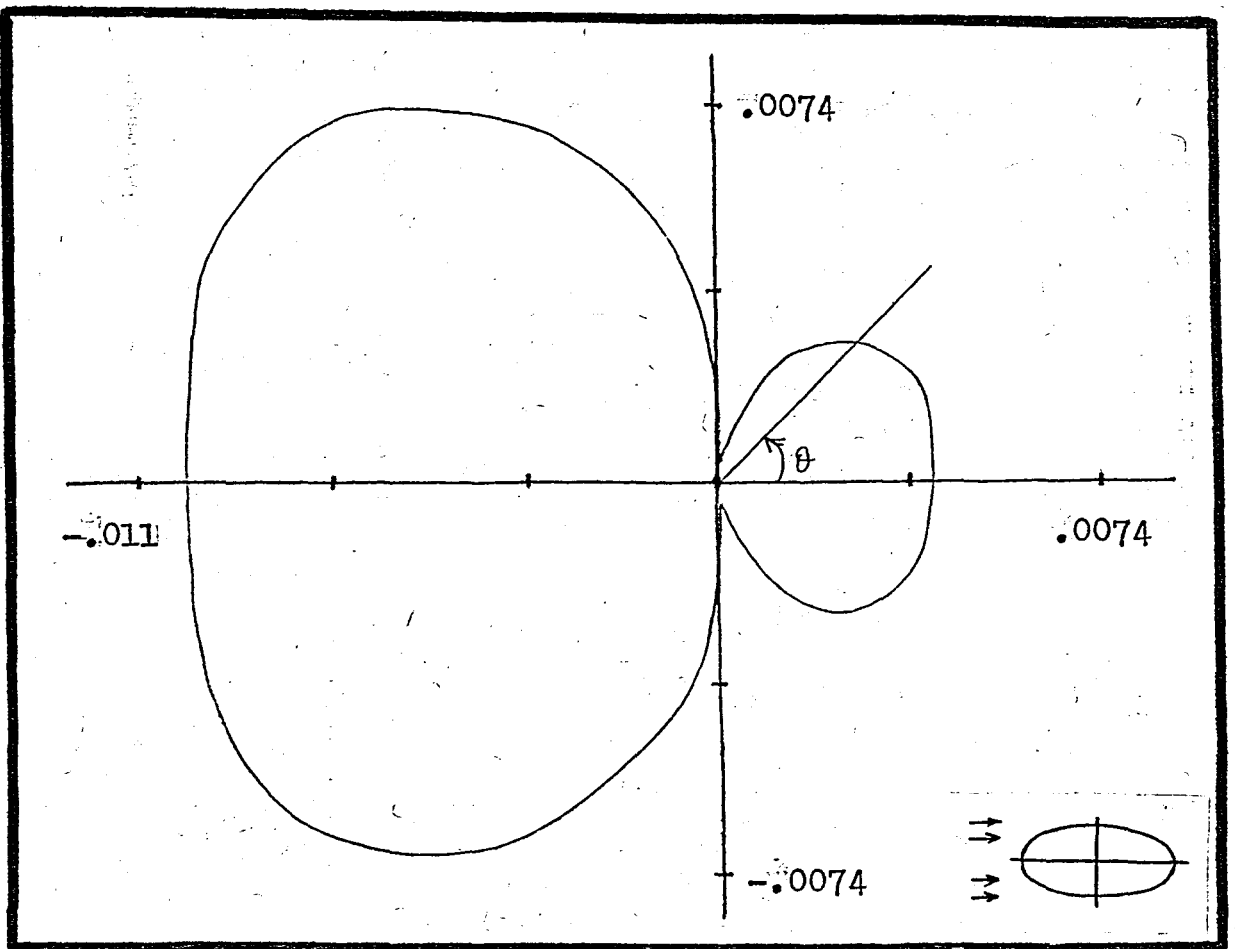


Figure 6(c) $k=0.5$, $a=1.0$, $b=0.5$

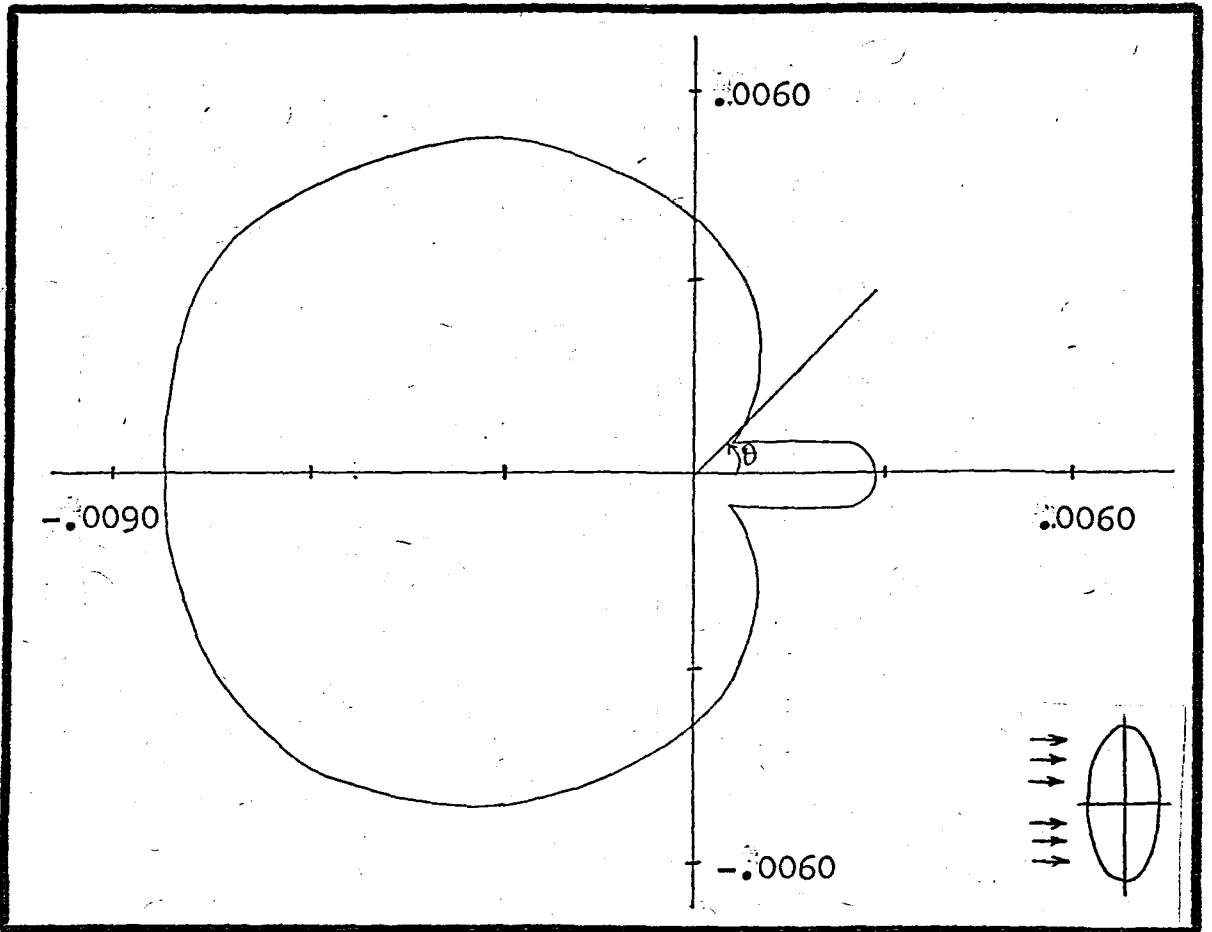
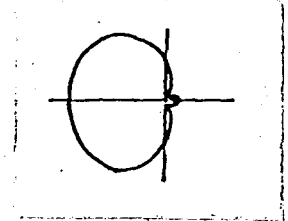
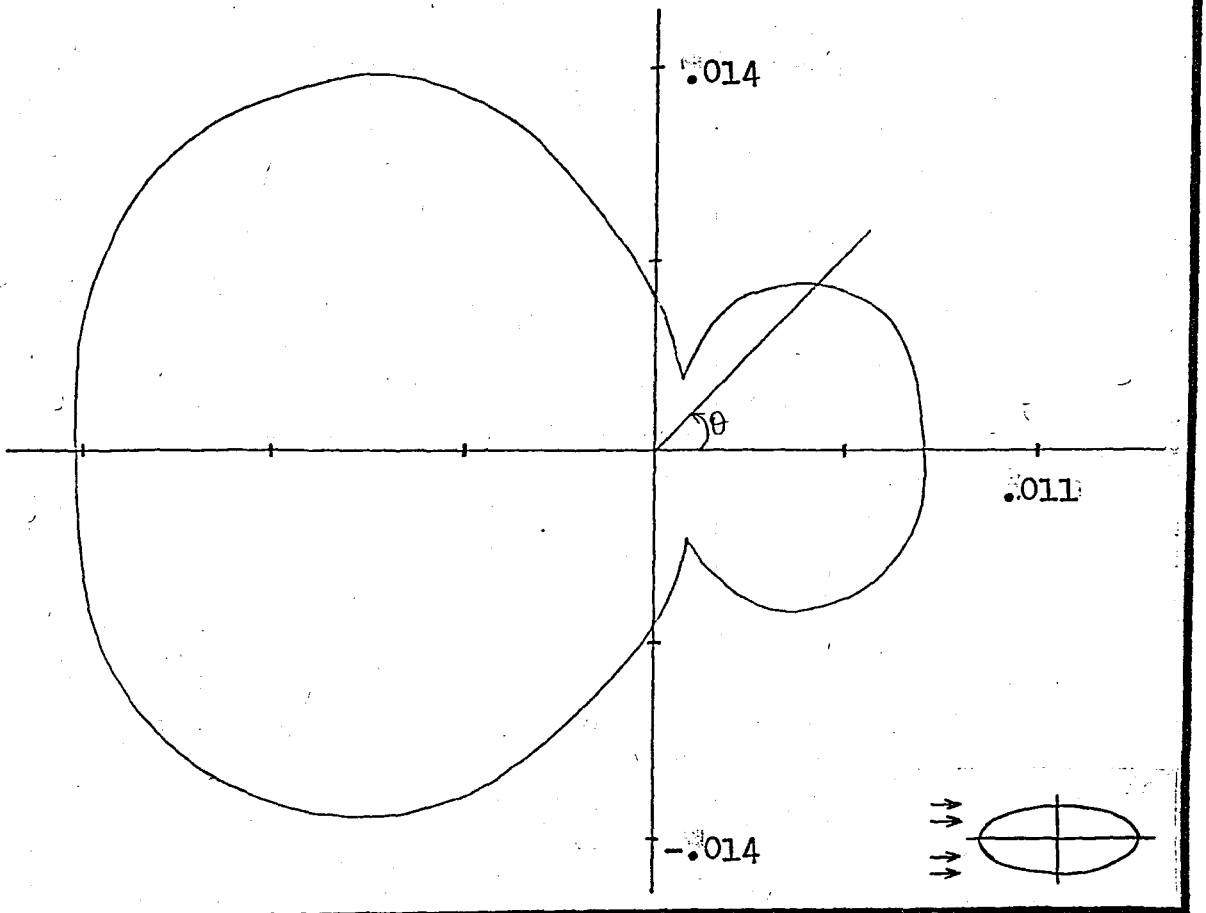
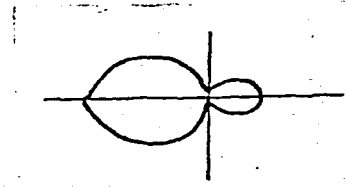


Figure 6(d) $k=0.5$, $a=0.5$, $b=1.0$



Exact solution [20]

Figure 6(e) $k=1.0$, $a=1.0$, $b=0.5$



Exact solution [20]

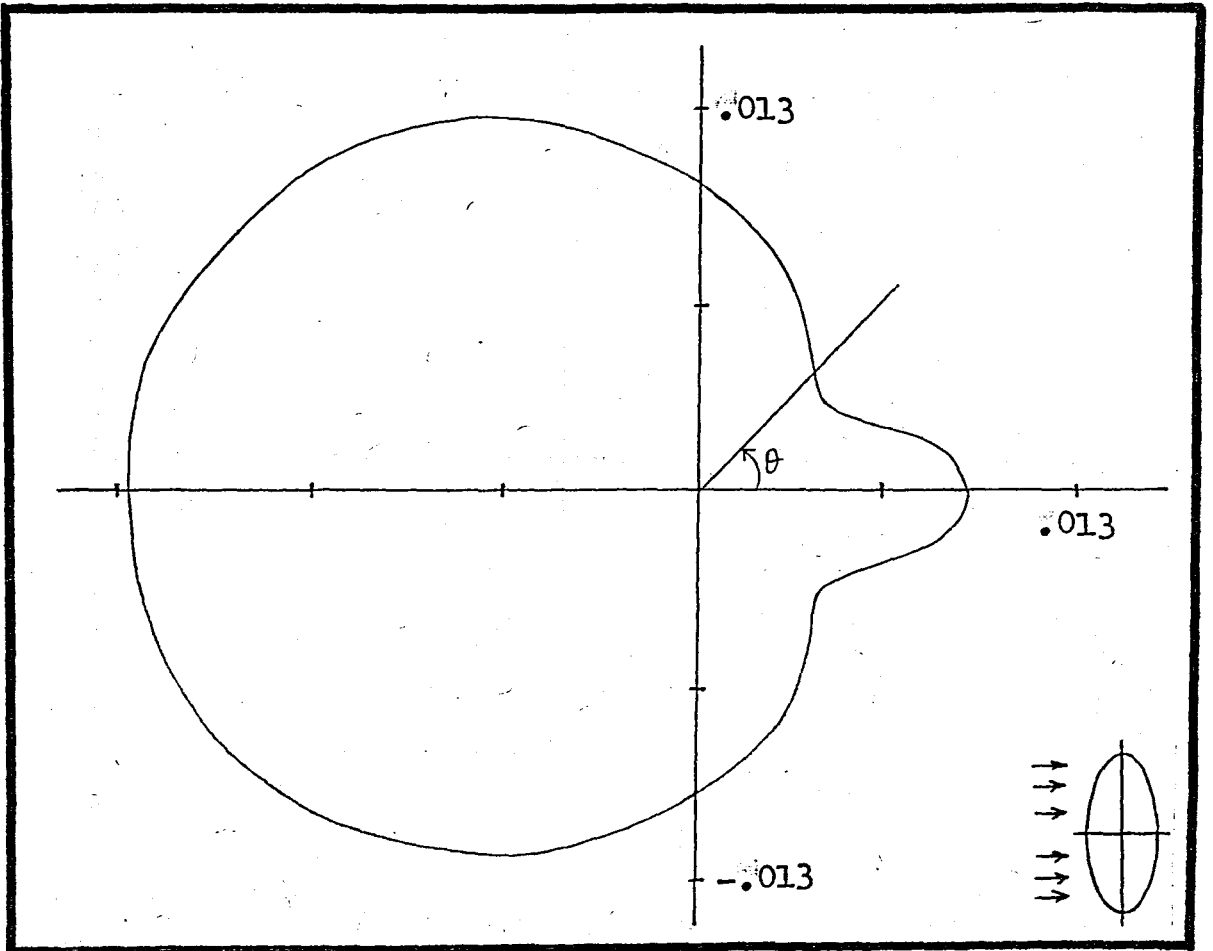
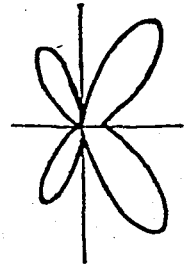


Figure 6(f) $k=1.0$, $a=0.5$, $b=1.0$



Exact solution [20]

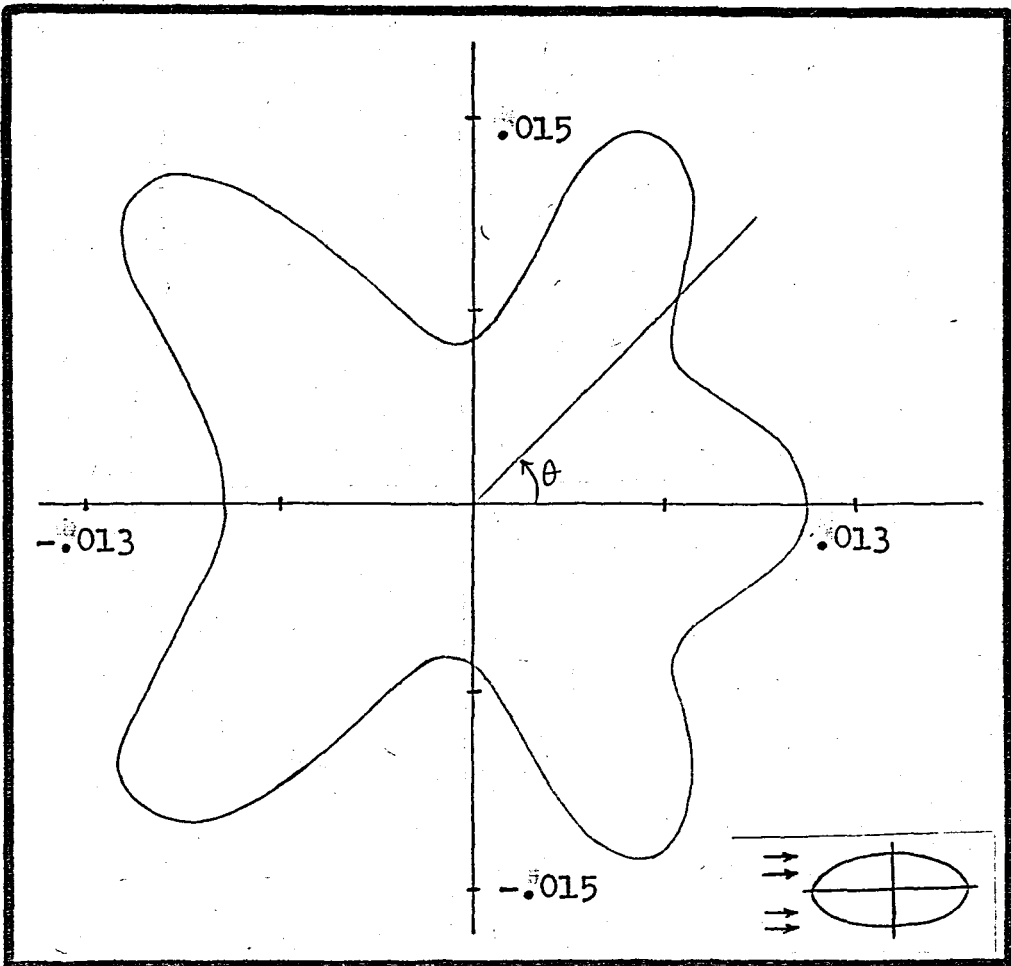


Figure 6(g) $k = 5.0$, $a = 1.0$, $b = 0.5$



Exact solution [20]

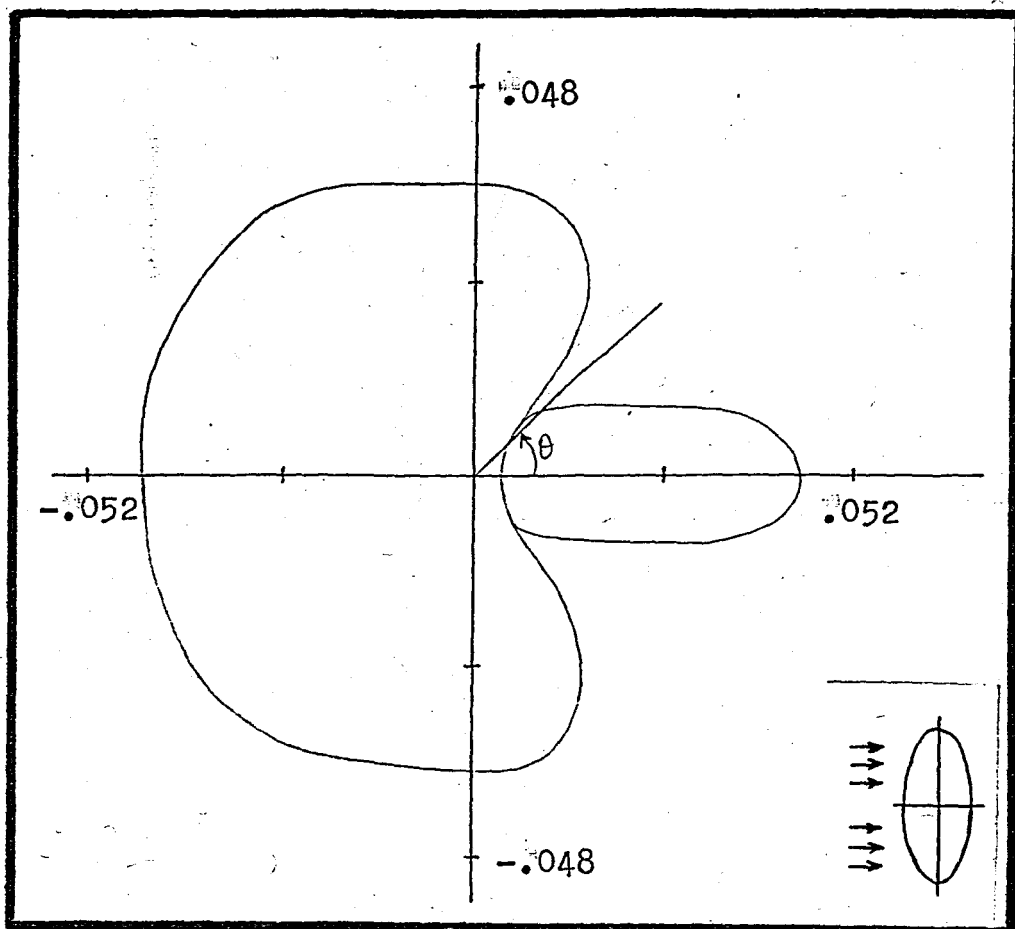
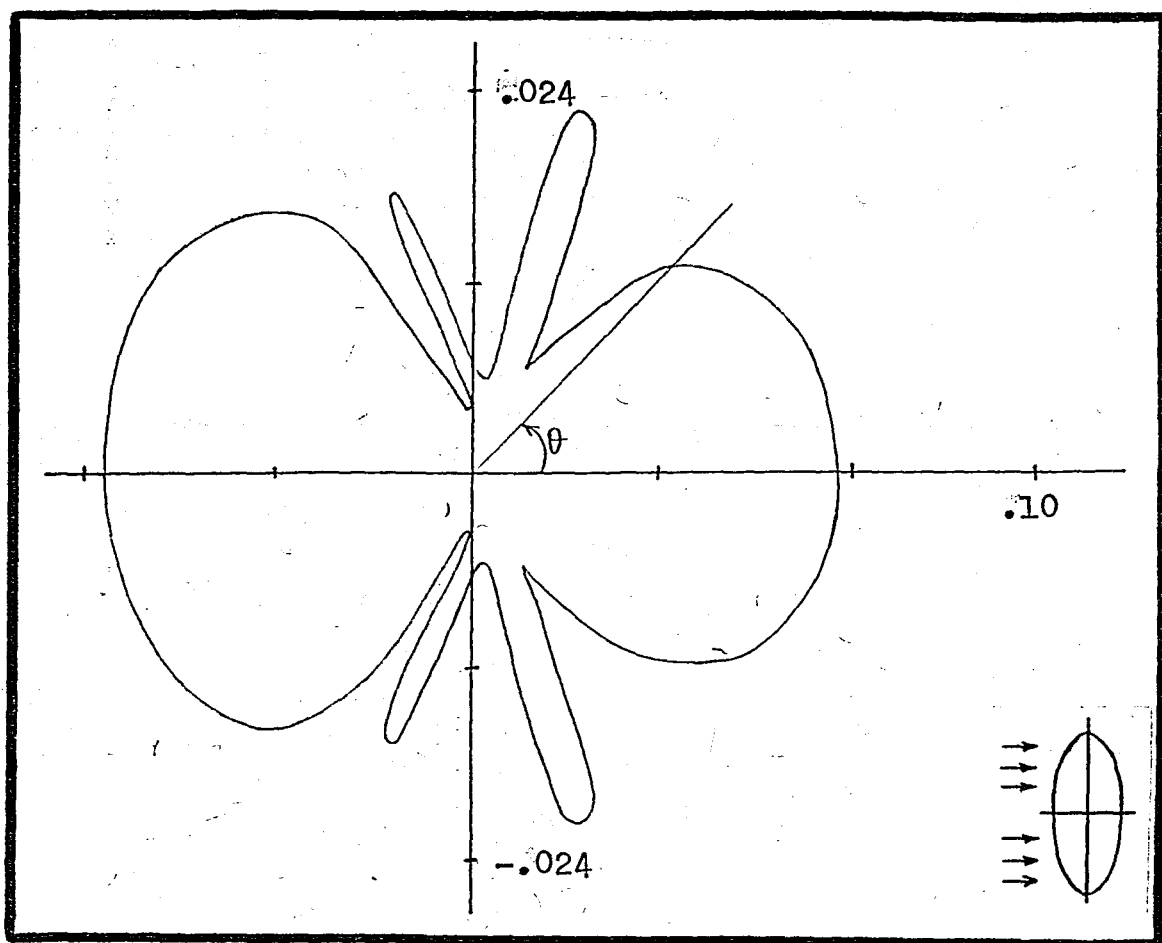
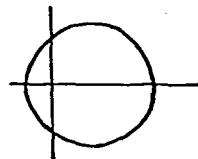


Figure 6(h) $k=5.0$, $a=0.5$, $b=1.0$

Exact solution [20]

Figure 6(1) $k=5.0$, $a=0.5$, $b=2.5$



Exact solution [20]

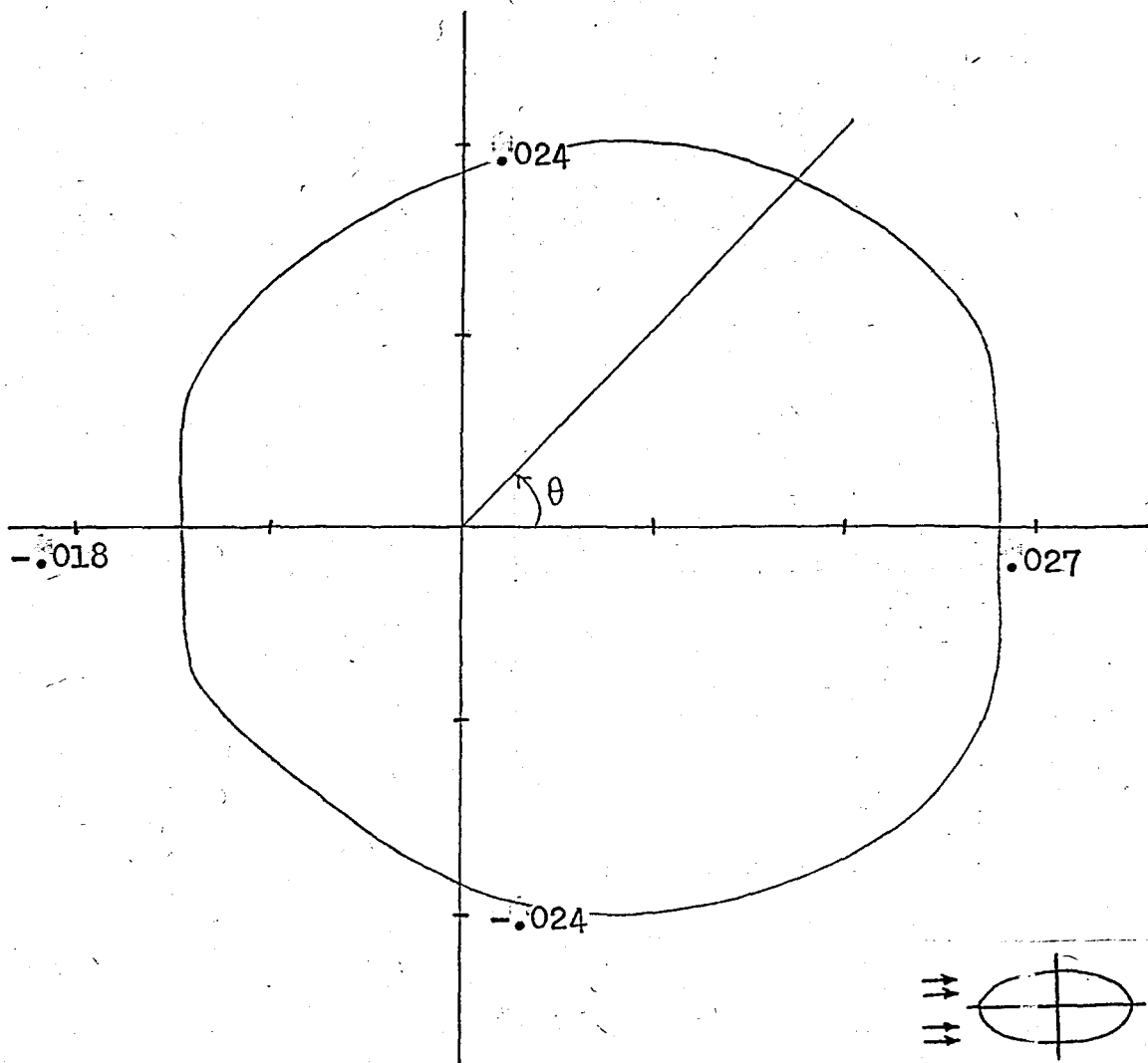
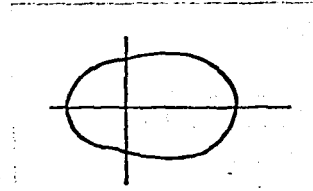
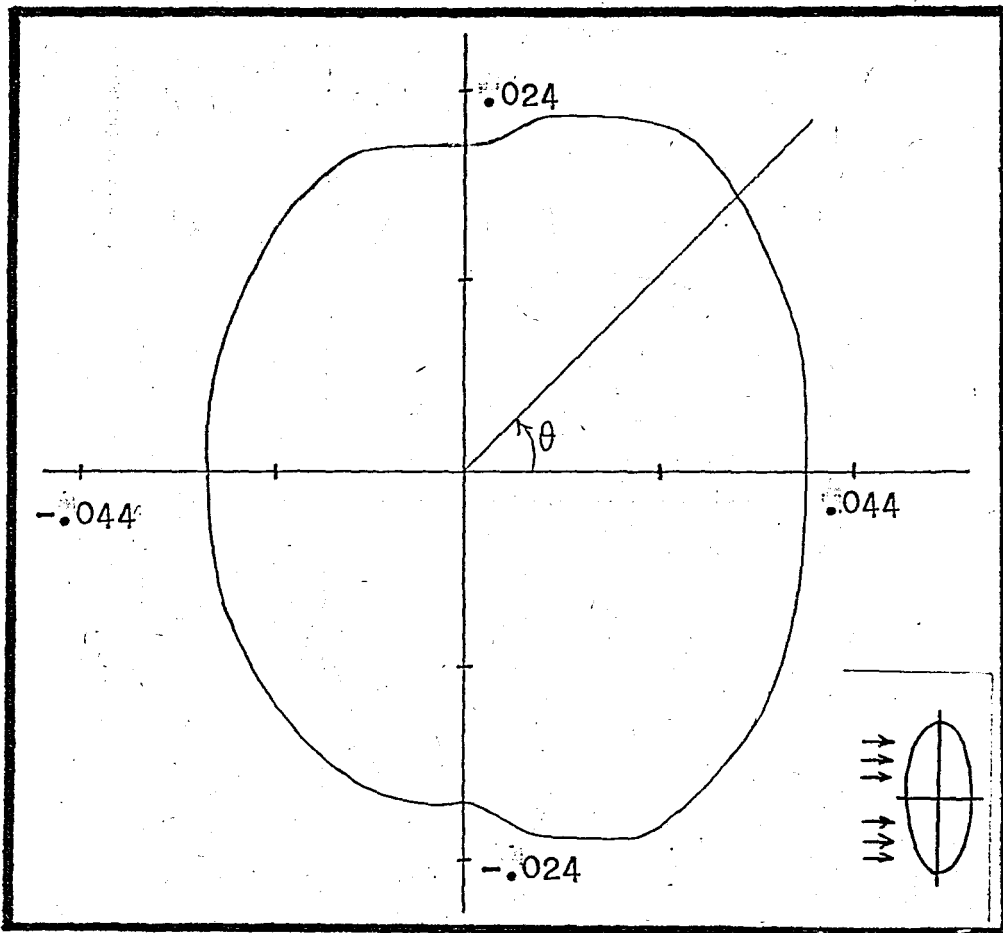


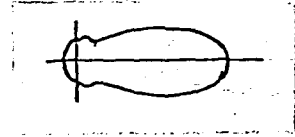
Figure 7 Far-field displacement due to the scattered wave field from a rigid elliptical inclusion.

7(a) $k=1.0$, $a=1.0$, $b=0.5$



Exact solution [20]

Figure 7(b) $k=1.0$, $a=0.5$, $b=1.0$



Exact solution [20]

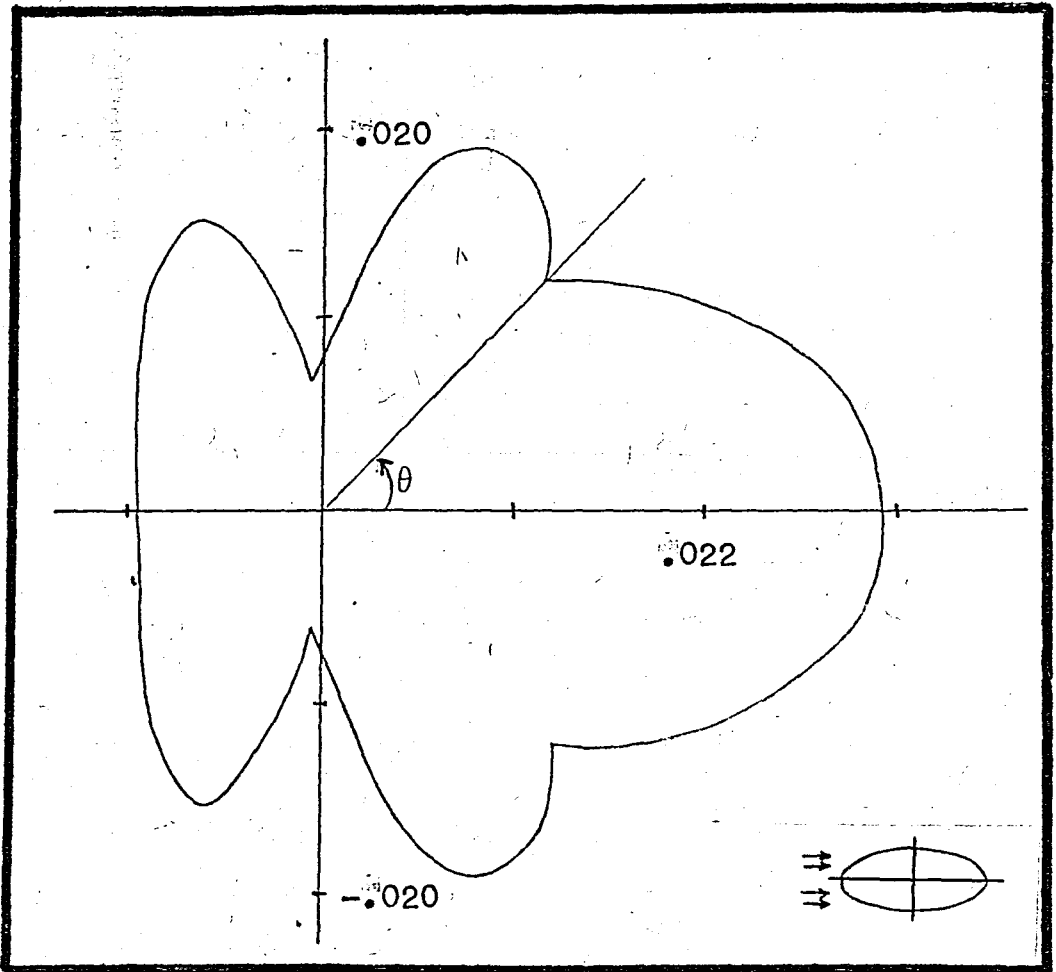


Figure 7(c) $k=5.0$, $a=1.0$, $b=0.5$

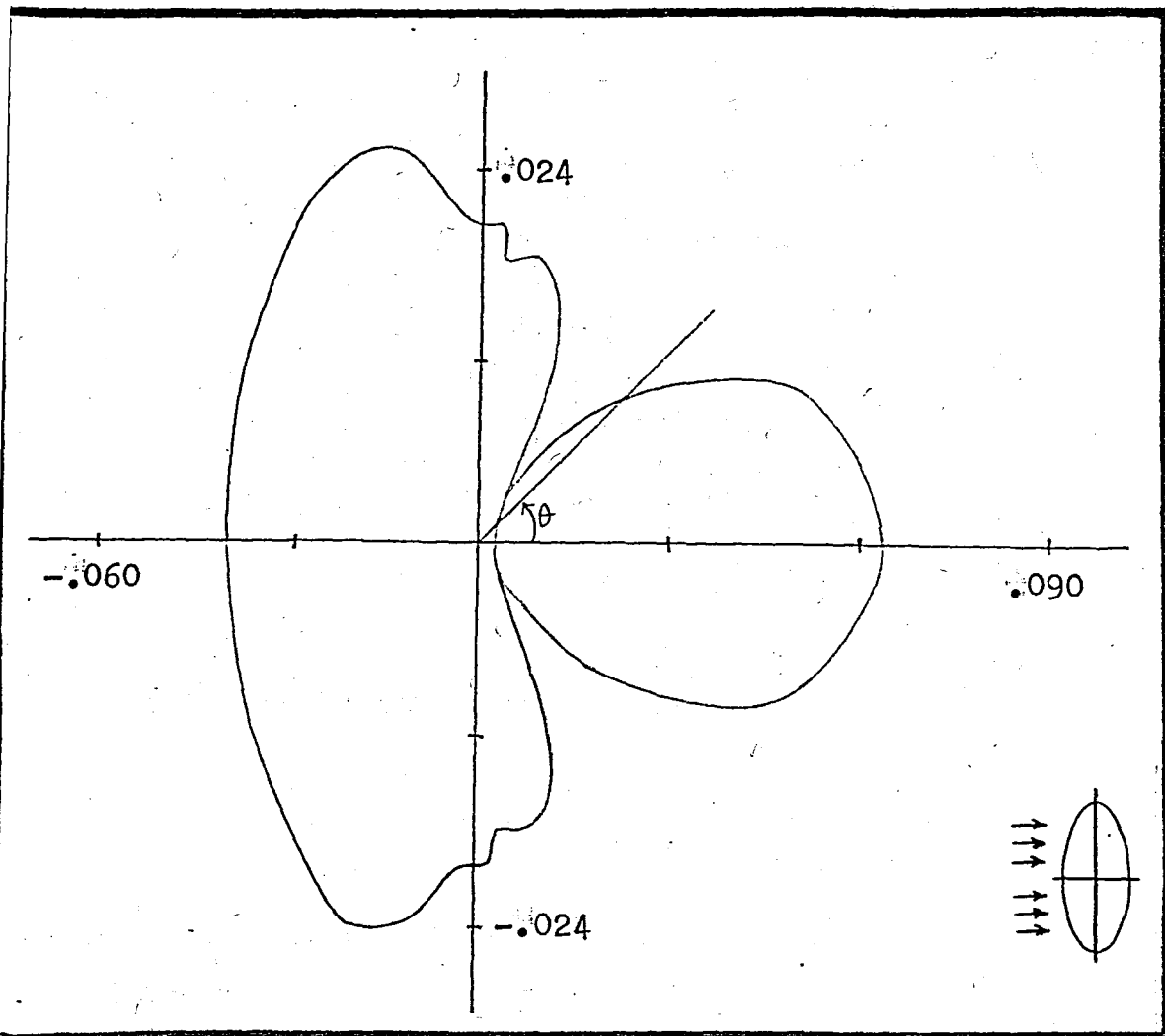
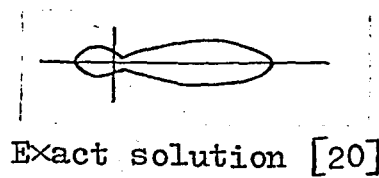


Figure 7(d) $k=5.0$, $a=0.5$, $b=1.0$

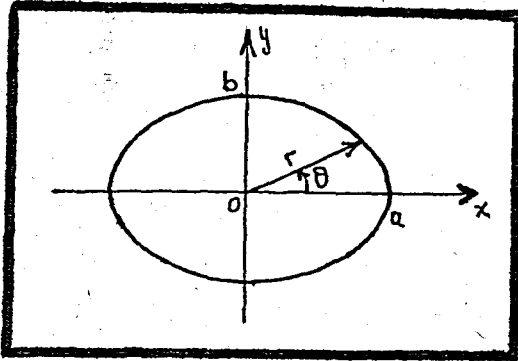
APPENDIX

The equation of an ellipse is

$$\frac{x^2}{a^2} + \frac{y^2}{b^2} = 1 \quad (\text{A.1})$$

where

$$x = r \cos \theta \quad \text{and} \quad y = r \sin \theta \quad (\text{A.2})$$



Equation (A.1) can also be written as

$$b^2 x^2 + a^2 y^2 = a^2 b^2$$

Substituting for x and y , the expressions in equation (A.2) and solving for r :

$$r = \frac{ab}{\sqrt{b^2 \cos^2 \theta + a^2 \sin^2 \theta}} = \frac{ab}{\sqrt{a^2 + (b^2 - a^2) \cos^2 \theta}} \quad (\text{A.3})$$

The derivative of r with respect to θ is:

$$\frac{dr}{d\theta} = - \frac{ab (a^2 - b^2) \cos\theta \sin\theta}{(b^2 \cos^2\theta + a^2 \sin^2\theta)^{3/2}} \quad (\text{A.4})$$

Arc length is given by

$$\frac{dS}{d\theta} = \sqrt{[x'(\theta)]^2 + [y'(\theta)]^2}$$

where prime indicates differentiation with respect to θ .

Using (A.2) $dS/d\theta$ can be found as

$$\frac{dS}{d\theta} = \sqrt{r'^2 + r^2}$$

Substituting equations (A.3) and (A.4) into (A.5), after simple algebra, one obtains

$$dS = ab \sqrt{\frac{a^4 \sin^2\theta + b^4 \cos^2\theta}{(a^2 \sin^2\theta + b^2 \cos^2\theta)^3}} d\theta \quad (\text{A.6})$$

It is known that

$$r = \sqrt{x^2 + y^2}$$

Hence

$$\begin{aligned}\nabla r &= \frac{\partial}{\partial x} \sqrt{x^2 + y^2} \underline{\hat{i}} + \frac{\partial}{\partial y} \sqrt{x^2 + y^2} \underline{\hat{j}} \\ &= \frac{x}{\sqrt{x^2 + y^2}} \underline{\hat{i}} + \frac{y}{\sqrt{x^2 + y^2}} \underline{\hat{j}}\end{aligned}\quad (\text{A.7})$$

Substituting

$$x = r \cos \theta \quad \text{and} \quad y = r \sin \theta$$

into equation (A.7)

$$\begin{aligned}\nabla r &= \frac{r \cos \theta}{\sqrt{r^2 \cos^2 \theta + r^2 \sin^2 \theta}} \underline{\hat{i}} + \frac{r \sin \theta}{\sqrt{r^2 \cos^2 \theta + r^2 \sin^2 \theta}} \underline{\hat{j}} \\ &= \cos \theta \underline{\hat{i}} + \sin \theta \underline{\hat{j}}\end{aligned}\quad (\text{A.8})$$

Since

$$\frac{x^2}{a^2} + \frac{y^2}{b^2} = 1$$

the unit outward normal is

$$\underline{\hat{n}} = \frac{\frac{2x}{a^2} \underline{\hat{i}} + \frac{2y}{b^2} \underline{\hat{j}}}{\sqrt{\frac{4x^2}{a^4} + \frac{4y^2}{b^4}}}$$

Using (A.2), the last equality becomes

$$\underline{\underline{n}} = \frac{b^2 \cos \theta \underline{\underline{i}} + a^2 \sin \theta \underline{\underline{j}}}{\sqrt{b^4 \cos^2 \theta + a^4 \sin^2 \theta}} \quad (\text{A.9})$$

Using (A.8) and (A.9), we can find

$$\frac{\partial r}{\partial n} = \underline{\underline{n}} \cdot \underline{\underline{\nabla}} r$$

$$= \frac{b^2 \cos \theta \underline{\underline{i}} + a^2 \sin \theta \underline{\underline{j}}}{\sqrt{b^4 \cos^2 \theta + a^4 \sin^2 \theta}} \cdot (\cos \theta \underline{\underline{i}} + \sin \theta \underline{\underline{j}})$$

$$= \frac{b^2 \cos^2 \theta + a^2 \sin^2 \theta}{\sqrt{b^4 \cos^2 \theta + a^4 \sin^2 \theta}} \quad (\text{A.10})$$

Setting $a=b$, one obtains $\partial S/\partial \theta$ and $\partial r/\partial n$ for the circle as

$$\frac{\partial S}{\partial \theta} = a \quad (\text{A.11})$$

$$\frac{\partial r}{\partial n} = 1 \quad (\text{A.12})$$

ACKNOWLEDGEMENTS

I take the opportunity to thank Dr.Ahmet Ceranođlu, Prof.Dr.Akın Tezel, Dođ.Dr.Başar Civelek and Prof.Dr.Atila Aşkar for their sincere cooperations and excellent supports throughout this work.

REFERENCES

- [1] Sezewa, Katsutada, "Scattering of Elastic Waves and Some Applied Problems", Bull. Earthquake Res. Inst., Vol. 3, Tokyo Imperial University, 1927, p. 19.
- [2] Harumi, K., "Scattering of Plane Waves by a Rigid Ribbon in a Solid", J. Appl. Phys., Vol. 32, 1961, p. 1488.
- [3] Mc Lachlan, N.W., Theory and Application of Mathieu Functions, Oxford University Press, London, 1951, p. 358.
- [4] Morse, P.M., and H. Feshbach, Methods of Theoretical Physics, Mc Graw-Hill Book Co., New York, 1953.
- [5] Rayleigh, Lord, "On the Incidence of Aerial and Electric Waves upon Small Obstacles in the Form of Ellipsoids or Elliptic Cylinders, and on the Passage of Electric Waves Through a Circular Aperture in a Conducting Screen", Phil. Mag., Vol. 44, 1897, p. 28. (Scientific Papers, Vol. 4, Cambridge University Press, 1903, p. 305)
- [6] Sieger, B. "Die Beugung einer ebenen elektrischen Welle an einem Schirm von elliptischem Querschnitt", Ann. Phys., Vol. 27, 1908, p. 626.
- [7] Morse, P.M., and P.J. Rubenstein, "Diffraction of Waves by Ribbons and Slits", Phys. Rev., Vol. 54, 1938, p. 895.
- [8] Bouwkamp, C.J., "Diffraction Theory", Reports on Progress in Phys., Vol. 17, 1954, p. 35.
- [9] Jones, D.S., The Theory of Electromagnetism, Pergamon Press, London, 1964, Chapter 8.
- [10] Barakat, Richard, "Diffraction of Plane Waves by an Elliptic Cylinder", J. Acoustical Soc. Amer., Vol. 35, 1963, p. 1990.

- [11] James Alan Cochran, The Analysis of Linear Integral Equations, Mc Graw-Hill Book Co., New York, 1972.
- [12] Tricomi, F. G., Integral Equations, Interscience Publishers, New York, 1957.
- [13] Roach, G. F., Greens Functions-Introductory Theory with Applications, Van Nostrand Reinhold Company, New York, 1970.
- [14] Pao, Y.-H., and Mow, C. C., Diffraction of Elastic Waves and Dynamic Stress Concentrations, Crane Russak-Adam Hilger, New York, 1973.
- [15] Chu, L. L., Çakmak, A., and Aşkar, A., "Born Approximation For Wave Scattering in Elastodynamics", ASME, New York, 1980.
- [16] Chu, L. L., Aşkar, A., Çakmak, A., "Scattering of Plane Strain P and S Waves by Cavities and Rigid Inclusions-The Born Approximation", Princeton University, 1980.
- [17] Achenbach, J. D., Wave Propagation in Elastic Solids, American Elsevier Pub. Co., New York, 1973.
- [18] Abramovitz, M. and Stegun, I. A., Handbook of Mathematical Functions, U.S. Government Printing Office, Washington, D.C., 1964.
- [19] Gradshteyn, I. S., Ryzhik, I. M., Table of Integrals Series and Products, Academic Press, New York, 1965.
- [20] Banaugh, R. P., Goldsmith, W., "Diffraction of Steady Acoustic Waves by Surfaces of Arbitrary Shape", J. Acoustical Soc. Amer., Vol. 35, 1963, p. 1590.